Fate of Photoexcited trans-Aminostilbenes

ARTICLE *in* JOURNAL OF PHOTOCHEMISTRY AND PHOTOBIOLOGY A CHEMISTRY · MAY 2015

Impact Factor: 2.5 · DOI: 10.1016/j.jphotochem.2015.05.031

2 AUTHORS, INCLUDING:

Che-Jen Lin

National Taiwan University

5 PUBLICATIONS **17** CITATIONS

SEE PROFILE

Journal of Photochemistry and Photobiology A: Chemistry 312 (2015) 107–120

Contents lists available at ScienceDirect

Journal of Photochemistry and Photobiology A: Chemistry

journal homepage: www.elsevier.com/locate/jphotochem

Invited feature article

Fate of photoexcited *trans*-aminostilbenes

Jye-Shane Yang*, Che-Jen Lin

Department of Chemistry, National Taiwan University, No. 1, Sec. 4, Roosevelt Road, Taipei 10617, Taiwan

ARTICLE INFO

Article history:
Received 17 February 2015
Received in revised form 24 March 2015
Accepted 25 May 2015
Available online 29 May 2015

Keywords:
Fluorescence
Trans-to-*cis* isomerization
TICT model
N-arylamino conjugation effect
Ortho–meta effect
Fluoroionophore

ABSTRACT

The decay pathways with relative quantum efficiencies for photoexcited *trans*-aminostilbenes in dilute organic solutions at ambient temperature are reviewed. Like the case of the parent *trans*-stilbene, fluorescence and the vinylene C=C torsion are two important decay pathways for *trans*-aminostilbenes. However, a new pathway, that is, formation of a TICT state by twisting the phenylene-amino C—N bond, dominates the excited-state deactivation of some *trans*-aminostilbenes in medium and/or highly polar solvents. On the basis of the quantum yields of fluorescence (Φ_f) and the *trans* → *cis* isomerization (Φ_{tc}) in solvents of different polarity, the TICT-forming activity of *trans*-aminostilbenes could be readily probed. The TICT states could be unambiguously characterized with ring-bridged model compounds, profiles of the emission spectra, and variable–temperature emission spectra. The interplay among fluorescence, the *trans* → *cis* isomerization, and the TICT state formation strongly depend on the nature and position of the amino group(s), the solvent polarity, and the other substituents that significantly perturb the steric and/or electronic properties. This provides a unique opportunity toward the design of novel fluorescent probes, light-emitting materials, and molecular switches.

1. Introduction

Trans-aminostilbenes are a class of π-donor–acceptor (D–A) systems that have been investigated as fluorescent probes [1–6], cell imaging dyes [7–9], and the active materials in a variety of optoelectronic devices such as organic light-emitting diodes [10,11], dye-sensitized solar cells [12–14], nonlinear optics [15–20], and molecular switches [21,22]. These applications are all associated with the electronically excited states, in which the lowest singlet excited state (S_1) possesses a significant degree of charge separation as a result of intramolecular charge–transfer (ICT) from the amino to the stilbene moiety upon photoexcitation. The polar ICT state corresponds spectroscopically to a high solvatofluorochromicity [23]. The ICT state could undergo two distinct types of adiabatic torsional relaxations: namely, the C=C torsion that forms a perpendicular ($^1p^*$) state and accounts for the *trans* → *cis* isomerization and the D–A torsion that forms a twisted intramolecular charge–transfer (TICT) state (Fig. 1). The interplay among fluorescence, photoisomerization, and TICT state formation strongly depends on the nature and position of the amino group, the steric and electronic impacts of substituents, and the solvent polarity. Since a fundamental understanding of the structure–activity relationship is essential for the design of novel aminostilbene-based dyes, our research group has been elucidating the effects of amino position, substituents, and solvent polarity on the fluorescence, photoisomerization, and TICT-forming activity of *trans*-aminostilbenes. This article will describe our previous efforts on this issue as well as related works by other groups. Unless otherwise mentioned, all the data and conditions for discussion in this article refer to those in dilute organic solutions and at ambient temperatures (295–298 K).

2. From *trans*-stilbene to *trans*-aminostilbenes: a general picture

Previous works on the parent *trans*-stilbene have paved an important foundation for understanding the photophysics and photochemistry of *trans*-aminostilbenes [24–28]. *Trans*-stilbene adopts a planar structure in the ground state, and torsions about the phenyl–vinylene C—C and the central vinylene C=C bonds encounter a barrier of ~4 and ~43 kcal/mol, respectively [29,30]. Photoexcitation of *trans*-stilbene ($^1t^*$) significantly weakens the bond order of the C=C bond such that the torsion barrier is largely diminished to 3.5 kcal/mol, which facilitates the *trans* → *cis* isomerization. As depicted in Fig. 2, the torsion reaches a conical intersection at an angle of ~90° called a phantom or perpendicular state ($^1p^*$). Internal conversion of the $^1p^*$ state leads to ^1p that is near the transition state of the *cis–trans* isomerization in the ground state. Because of the small energy difference between the *trans* and *cis* isomers, the driving force from ^1p to either isomer is

* Corresponding author. Tel.: +886 2 33661649; fax: +886 2 33668681.
E-mail address: jsyang@ntu.edu.tw (J.-S. Yang).

http://dx.doi.org/10.1016/j.jphotochem.2015.05.031
1010-6030/

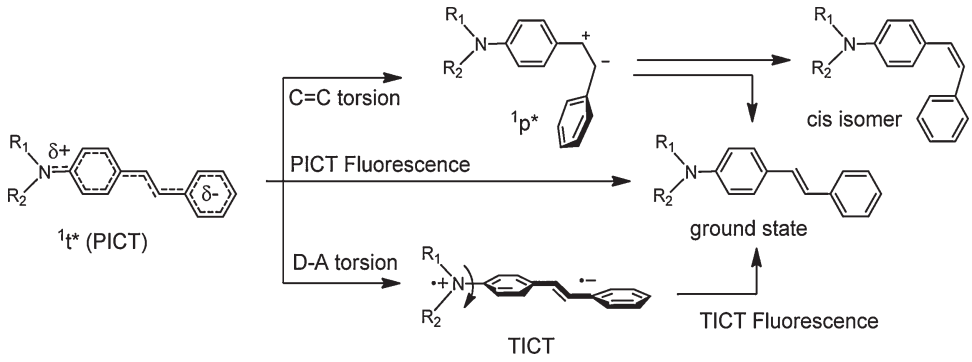

Fig. 1. Three major deactivated channels of photoexcited *trans*-aminostilbenes as represented by a para system.

similar (i.e., ~50% partition probability for each). Consequently, the determined *trans* → *cis* isomerization quantum yield (Φ_{tc}) is approximately half of the quantum efficiency for the C=C torsion (i.e., $\Phi_{\text{torsion of C=C}} \approx 2\Phi_{tc}$). The singlet-state C=C torsion dominates the photochemistry of *trans*-stilbene in solutions, resulting in low fluorescence quantum efficiencies ($\Phi_f \leq 5\%$). Constraint of the C=C torsion in favor of fluorescence has been demonstrated with *trans*-stilbene in spatially confined molecular hosts [31,32] or rigid media [33,34]. The sum of $\Phi_f + 2\Phi_{tc}$ is close to unity in all non-viscous solvents, indicating that other decay channels such as intersystem crossing ($^1t^* \rightarrow {}^3t^*$) and internal conversion ($^1t^* \rightarrow {}^1t$) of $^1t^*$ are relatively unimportant. Nevertheless, studies on photosensitized *trans*-stilbene show that the C=C torsion is even more favorable in the lowest triplet excited state (T_1) than in the S_1 state, as the $^3t^* \rightarrow {}^3p^*$ process is essentially barrierless and the intersystem crossing from $^3p^*$ to ^1p is much more efficient than that from $^3t^*$ to ^1t [25–28].

Substituent effects on the fluorescence and *trans* → *cis* isomerization of *trans*-stilbene are well-documented [25]. Substitutions on the phenyl ring generally retain the feature of low Φ_f and high Φ_{tc}, although the isomerization reaction might shift from S_1 to T_1 with certain substituents such as nitro, carbonyl, bromo, and iodo groups [35]. Regardless of the mechanism being singlet or triplet, the high efficiency of *cis–trans* photoisomerization renders stilbene systems good candidates as light-gated molecular switches [36,37]. On the other hand, substituents that suppress the C=C torsion in favor of fluorescence are desirable for applications as fluorescent probes or light-emitting materials. In this context, *trans*-aminostilbenes are particularly interesting, because certain amino groups could largely raise the singlet-state C=C torsion barrier such that the torsional process could become slower than the fluorescence decay (vide infra). However, introducing a strong electron-donating amino group to *trans*-stilbene simultaneously imposes an ICT character for this π system, which might induce a new decay pathway: namely, formation of a TICT state. In this context, whether a TICT state is effectively populated becomes the most critical question in understanding the photochemistry of *trans*-aminostilbenes.

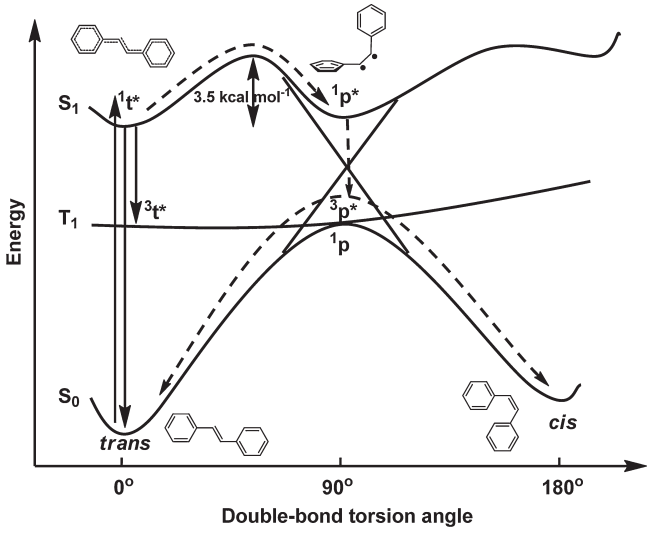

Fig. 2. Simplified potential energy surface diagram for the C=C torsion pathways of *trans*-stilbene.

3. TICT state of trans-aminostilbenes

3.1. Earlier TICT model of trans-aminostilbenes

The TICT model for D–A systems originated from the observation of dual emission at ~350 and ~550 nm for 4-(*N*,*N*-dimethylamino)benzonitrile (DMABN) in acetonitrile (Chart 1) [38,39]. The short- and long-wavelength emission bands have been attributed to the so-called locally excited (LE) and ICT states, respectively, on the basis of the size and direction of transition dipole moments. Whereas the LE state has a dipole moment of ~9.7 D and the LE emission is short-axis polarized, the ICT state has a dipole moment as large as ~17 D with the emission being long-axis polarized [40]. The precursor–successor relationship between the LE and the ICT states is well established, but the structural nature of the ICT state has been controversial [41]. The two most often discussed models differ mainly in the torsion angle about the phenylene-amino C_{ph}—N bond: the ICT state that possesses a small torsion angle corresponds to a planar ICT (PICT) state, and the one with a large torsion angle is called a TICT state (Fig. 3). A PICT state

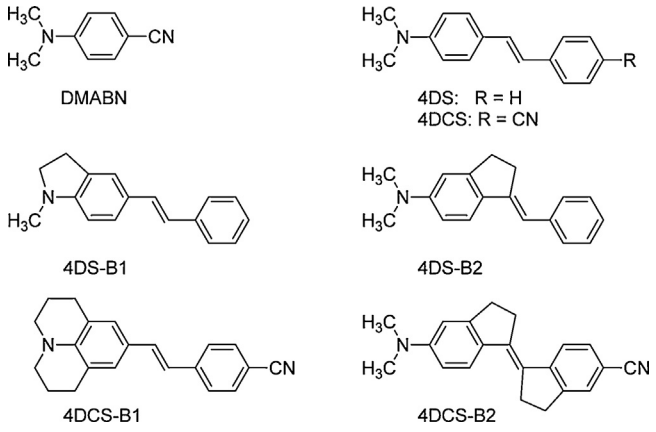

Chart 1. Structures of DMABN and *trans*-4-(*N*,*N*-dialkylamino)stilbenes.

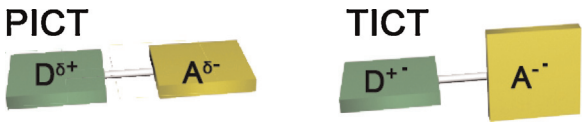

Fig. 3. Schematic representation of the structural and electronic nature of a PICT (left) and TICT (right) state.

allows charge delocalization over the amino donor (D) and the benzonitrile acceptor (A). In contrast, a TICT state allows full charge separation between the D and A groups such that the molecular dipole moment is largely increased. The gain of solvation stabilization in polar solvents provides the driving force for the formation of a TICT state. Therefore, formation of a TICT state would be unfavorable for D–A systems in nonpolar solvents.

The TICT-forming argument on *trans*-aminostilbenes was first proposed for *trans*-4-(*N,N*-dimethylamino)-4′-cyanostilbene (4DCS) [42–45], which could be considered as a π-extended DMABN by replacing the phenylene group with a stilbene group. Interestingly, the TICT state proposed for 4DCS is not from the torsion of the phenylene-amino C_{ph}—N bond but that of the vinylene–anilino C_v—C_{an} bond. Such a TICT model comes from the comparison of 4DCS with the ring-bridged analogs 4DCS-B1 and 4DCS-B2 (Chart 1), in which rotation about the C_{ph}—N and C_v—C_{an} bonds is inhibited, respectively. A dramatic fluorescence quenching observed for 4DCS-B2 but not for 4DCS-B1 relative to 4DCS was the basis for the TICT argument; occurrence of the C_v—C_{an} torsion was believed to be responsible for a stronger fluorescence of 4DCS and 4DCS-B1 relative to 4DCS-B2. The same studies on *trans*-4-(*N,N*-dimethylamino) stilbene (4DS) and the corresponding model compounds 4DS-B1 and 4DS-B2 also led to the same TICT model for 4DS [46].

However, the above TICT model for 4DCS and 4DS has been severely challenged [47–49,50]. For example, the Φ_f of 4DCS and 4DS is of little or no dependence of the solvent polarity, which conflicts with the solvation-driven TICT state formation. In addition, the argument of a larger Φ_f value for the TICT than the PICT state conflicts with a larger transition moment expected for the latter in terms of the symmetry of orbitals. Although dual fluorescence is not a prerequisite to argue for the formation of a TICT state, the lack of dual emission for 4DCS and 4DS in all the investigated solvents is also different from the case of DMABN. Indeed, the results of our works do not support the above-proposed TICT model for 4DCS and 4DS (vide infra).

3.2. Strategy for probing the TICT candidates of trans-aminostilbenes

The controversy of the TICT vs. PICT state for DMABN and 4DCS reveals the difficulties in the identification and characterization of a TICT state merely by spectroscopic analysis. In this context, we have utilized a physical organic approach to elucidate the TICT state of *trans*-aminostilbenes. Our approach relies on the fact that $\Phi_f + 2\Phi_{tc} \approx 1.0$ holds for most of the known *trans*-stilbenes, indicating that decay channels other than fluorescence and the C=C torsion are generally negligible for a planar $^1t^*$ state [24,25,27,28]. We argued that formation of a TICT state from either the Franck–Condon ICT state or the relaxed planar $^1t^*$ (i.e., PICT) state of *trans*-aminostilbenes is a new decay channel that competes with the fluorescence and the C=C torsion. Therefore, the relationship of $\Phi_f + 2\Phi_{tc} << 1.0$ should be observed for TICT-forming candidates of *trans*-stilbene systems.

The above argument was indeed established with a series of *trans*-4-(*N*-arylamino)stilbenes **p1*R*** (Chart 2), in which ***R*** denotes the substituent in the para position of the *N*-aryl group [51]. Among the seven compounds, two distinct types of excited-state behavior were recognized. The first type is performed by the group

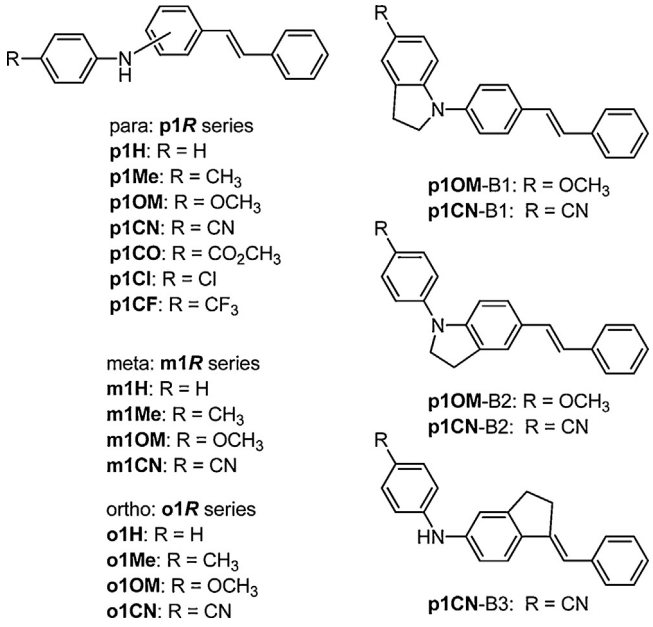

Chart 2. Structures of *trans*-2-, -3-, and -4-(*N*-arylamino)stilbenes and ring-bridged derivatives of the para system.

of **p1*R*** with a methyl (**p1Me**), hydrogen (**p1H**), chloro (**p1Cl**), or trifluoromethyl (**p1CF**) substituent. This group conforms to the common behavior of *trans*-stilbenes of $\Phi_f + 2\Phi_{tc} \approx 1.0$ in both nonpolar and polar solvents (note that values in the range 0.80–1.20 were considered to be near unity to accommodate the experimental uncertainty of both the Φ_f and Φ_{tc} data) [51,52]. The other group consisting of **p1*R*** with a methoxy (**p1OM**), cyano (**p1CN**), or methoxycarbonyl (**p1CO**) substituent displays the behavior of $\Phi_f + 2\Phi_{tc} \approx 1.0$ only in nonpolar solvents such as hexane but not in more polar solvents such as THF and acetonitrile. The value of $\Phi_f + 2\Phi_{tc}$ decreases with increasing the solvent polarity and reaches a value lower than 0.10 in acetonitrile. The dependence of Φ_f on the solvent polarity is even more pronounced, in which the value in hexane is larger than in acetonitrile by more than 50 folds. Such a solvent polarity effect on Φ_f and Φ_{tc} is consistent with the expectation of forming a TICT state in acetonitrile but not in hexane, and the diminishment of Φ_f in polar solvents is also consistent with the forbidden nature of optical transition for a TICT state. These features render the three *trans*-aminostilbenes **p1OM**, **p1CN**, and **p1CO** promising TICT-forming candidates.

3.3. New TICT model of trans-aminostilbenes

The formation of a TICT state for **p1OM**, **p1CN**, and **p1CO** in polar solvents is further corroborated by several other observations. First, dual fluorescence is present for **p1CN** and **p1CO** in acetonitrile (Fig. 4), attributable to the emission of the PICT and TICT states. Although **p1OM** displays only a single broad fluorescence band in acetonitrile, the unusual broadening of the fluorescence spectrum is indicative of unresolved PICT and TICT emission bands. The fluorescence half-bandwidth ($\Delta\nu_{1/2}$), which is ~6200 cm^{-1} for **p1OM** and ~8100 cm^{-1} for **p1CN**, provides a clue to the difference in energy between the PICT and TICT emission bands. In contrast, no evidence of dual emission could be identified for the normal group of **p1Me**, **p1H**, **p1Cl**, and **p1CF**, which possess a $\Delta\nu_{1/2}$ value of 3900 cm^{-1} or less.

Second, the relationship $\Phi_f + 2\Phi_{tc} \approx 1.0$ is recovered when the D–A bond torsion is inhibited by ring bridging (e.g., **p1OM**-B2 and **p1CN**-B1). In contrast, the behavior of $\Phi_f + 2\Phi_{tc} << 1.0$ is retained

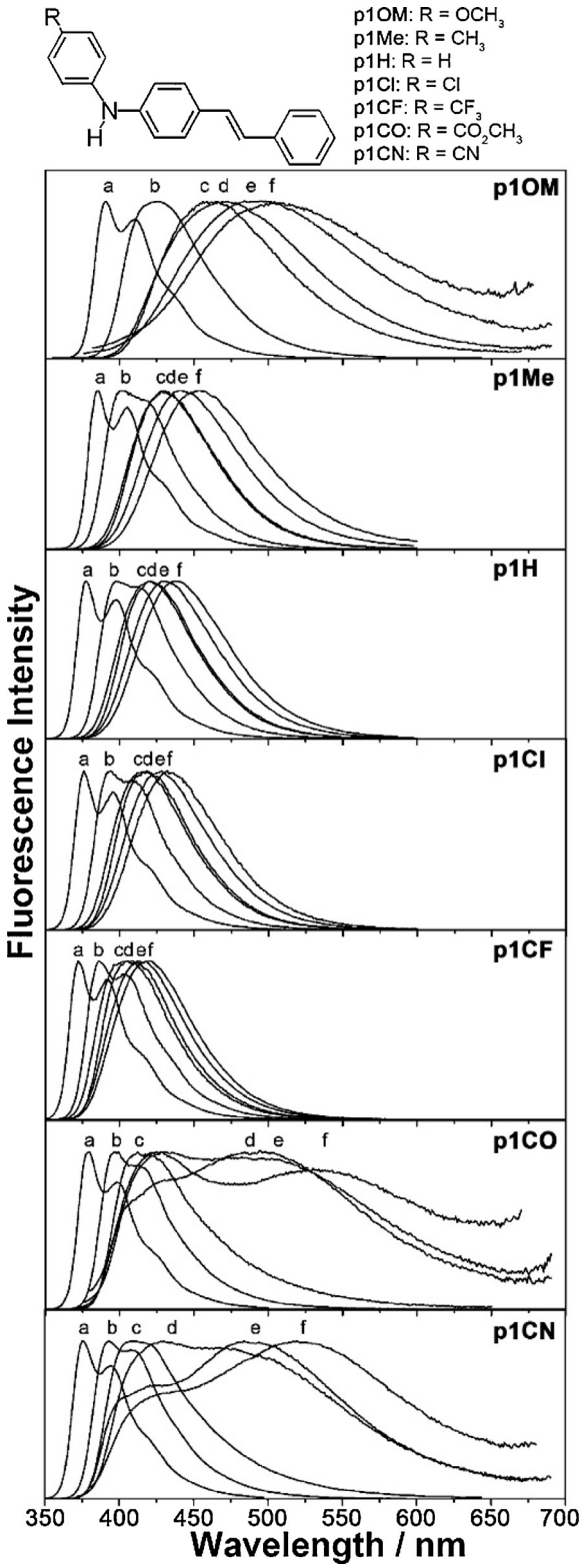

Fig. 4. Normalized fluorescence spectra of **p1*R*** in (a) hexane, (b) toluene, (c) THF, (d) dichloromethane, (e) acetone, and (f) acetonitrile. Modified from Ref. [51].

when the other unrelated single bonds (e.g., **p1OM**-B1, **p1CN**-B2, and **p1CN**-B3) are constrained. These ring-bridged model compounds not only corroborate the formation of a TICT state but also pinpoint the bond that twists (Fig. 5). In the case of **p1OM**, the bond that twists is the stilbene–arylamino C—N bond, but it is the benzonitrile–stilbeneamino C—N bond for the cases of **p1CN** and **p1CO**. The TICT state of **p1CN** resembles that of DMABN by having the benzonitrile group as the acceptor unit, indicating that an *N*-stilbeneamino donor is as good as a dimethylamino group to induce the D–A torsion. For comparison, *N*-methylaminobenzonitrile (MABN) does not form a TICT state under the same solvent conditions [53]. Despite the distinct role of the stilbene moiety in the TICT states of **p1OM** and **p1CN**, namely, it is in the acceptor moiety in **p1OM** but in the donor group in **p1CN**, the spectroscopic and photochemical behavior of the two types of TICT states are very similar. In particular, the low Φ_{tc} in associated with the TICT state formation shows that the deactivation of the TICT states is decoupled with the C=C torsion, regardless of the stilbene group being in the D or the A group.

The response of fluorescence intensity to the change of temperatures provides another evidence for the TICT argument (Fig. 6). For the parent *trans*-stilbene and TICT-free *trans*-aminostilbenes, increasing the temperature favors the activated reaction of the C=C torsions and thus decreases the fluorescence intensity. However, an opposite behavior was observed for the TICT-forming **p1CN** and **p1OM** in acetonitrile. This reflects that the TICT → PICT reversion has occurred and is faster than the PICT → ^{1}p* reaction upon increasing the temperature. The reversibility observed for the D–A torsion but not for the C=C torsion relies on the fact that deactivation of the TICT state is much slower than that of the ^{1}p* state. A simplified energy level diagram is shown in Fig. 7. However, it should be noted that this phenomenon (Fig. 6) is not a prerequisite to argue for a TICT state formation, because the temperature effect on the PICT → ^{1}p* conversion could be larger than on the TICT → PICT reversion. One such example will be shown later.

With the above TICT behavior in mind, the previously proposed TICT model for 4DCS and 4DS could be abandoned. One of the obvious shortages is the lack of sensitivity of Φ_f to solvent polarity. In addition, their fluorescence spectra resemble those of the TICT-free group of **p1*R*** instead of **p1OM** or **p1CN**. Moreover, the origin of lower Φ_f for 4DCS-B2 and 4DS-B2 than the parent compounds and 4DCS-B1 and 4DS-B1 is simply a consequence of the ring-bridging substituent effect that enhances the Φ_{tc} when the vinylene α carbon is alkyl substituted. This phenomenon was also found for the cases of **p1*R***. For example, in hexane the Φ_f of **p1CN**-B3 (0.32) is lower than **p1CN** (0.75), **p1CN**-B1 (0.81), and **p1CN**-B2 (0.75), but the Φ_{tc} of **p1CN**-B3 (0.30) is larger than **p1CN** (0.16) such that both **p1CN** and **p1CN**-B3 hold the relationship $\Phi_f + 2\Phi_{tc} \approx 1.0$. Apparently, the failure of the previously proposed TICT model for 4DCS and 4DS comes from the negligence of the nonradiative *trans* → *cis* isomerization process. We would like to emphasize that any proposed photodynamic model for stilbene derivatives would be jeopardized if the photoisomerization reaction was not taken into account. Our results also show that formation of a TICT state is not necessarily a favorable decay pathway for a D–A system.

4. Fluorescence-enhancing amino substituent effects

4.1. The N-arylamino conjugation effect

The success in characterizing the TICT state of *trans*-aminostilbenes with **p1*R*** relies on two important facts: (1) both TICT-free and TICT-forming compounds are simultaneously present for comparison and cross-referencing (vide supra), and (2) formation of a low-emissive TICT state can be readily recognized on going from nonpolar to polar solvents owing to a large drop of Φ_f. More specifically, the Φ_f of **p1*R*** in hexane is in the range 0.51–0.75 but it becomes less than 0.01 in acetonitrile when a TICT state is formed, leading to a decrease of Φ_f by more than 50 folds on going from hexane to acetonitrile. For comparison, the TICT-free group of **p1H**, **p1Me**, **p1Cl**, and **p1CF** maintains a significant size of Φ_f (0.25–0.43)

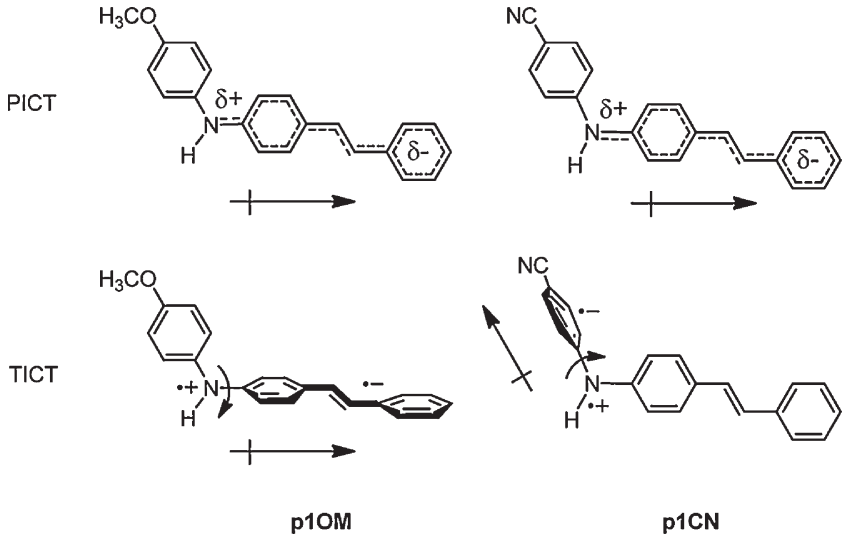

Fig. 5. The PICT and TICT states proposed for **p1OM** and **p1CN**. The acceptor group is drawn to be twisted from the plane of paper for the TICT states. The arrows indicate the polarization direction.

even in acetonitrile. In the plots of Φ_f against the solvent polarity parameter E_T (30), the TICT-forming systems display a sigmoidal curve but a linear correlation is present for the TICT-free systems (Fig. 8).

The strong fluorescence of **p1*R*** originates from the *N*-arylamino substituents that substantially raises the singlet-state C=C torsion barrier and thus decreases the C=C torsion efficiency. It is known that the C=C torsion barrier is ~3.5 kcal/mol for *trans*-stilbene [24]. A similar value of 3.6 kcal/mol was also determined for the case of *trans*-4-aminostilbene (4AS) and its *N*,*N*-dimethyl derivative 4DS [54,55]. However, the C=C torsion barriers are 4.9 and 7.4 kcal/mol for **p1H** and **p1CN**, respectively, in hexane [52,56]. The *N*-aryl substituent effect on raising the singlet-state C=C torsional barrier could be interpreted with the resonance structures of the $^1t^*$ and $^1p^*$ states. As illustrated with **p1H**, the *N*-phenyl group provides an additional resonance form (i.e., structure A in Scheme 1) for the $^1t^*$ state but not for the $^1p^*$ state. This corresponds to a larger stabilization of the $^1t^*$ state relative to the $^1p^*$ state. According to the Hammond postulate, lowering the energy of reactants ($^1t^*$) without changing the position of products ($^1p^*$) would raise the activation energy for the reaction (Fig. 9).

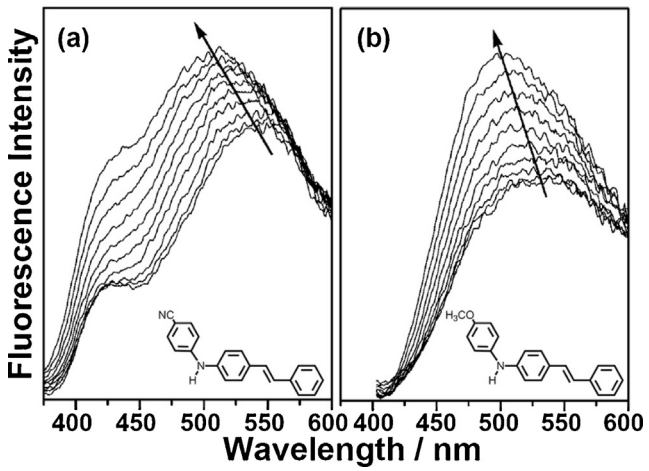

Fig. 6. Temperature-dependent fluorescence spectra of (a) **p1CN** and (b) **p1OM** in acetonitrile recorded at intervals of 10 °C between −40 and 50 °C. The arrows indicate the direction of fluorescence response upon raising temperature. Modified from reference [51].

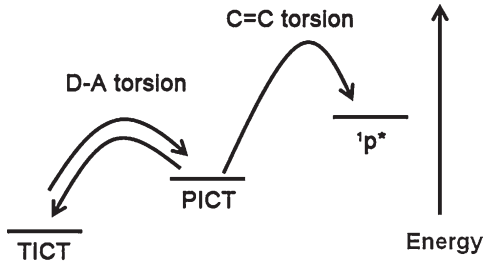

Fig. 7. Simplified energy level diagram of PICT, TICT and $^1p^*$ states.

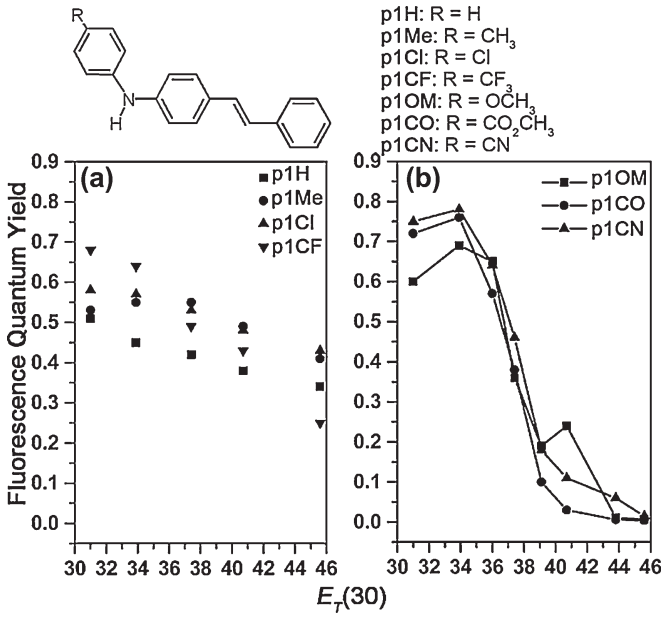

Fig. 8. Plots of the fluorescence quantum yield (Φ_f) against the solvent parameter E_T(30) for the series of **p1*R***. The solvents [E_T(30)] are (from left to right) hexane [31.0], toluene [33.9], THF [37.4], CH_2Cl_2 [40.7] and acetonitrile [45.6] for both plots (a) and (b), and three more solvents, 1,4-dioxane [36.0], $CHCl_3$ [36.0], and DMF [43.8], were added for plot (b). Modified from Ref. [51].

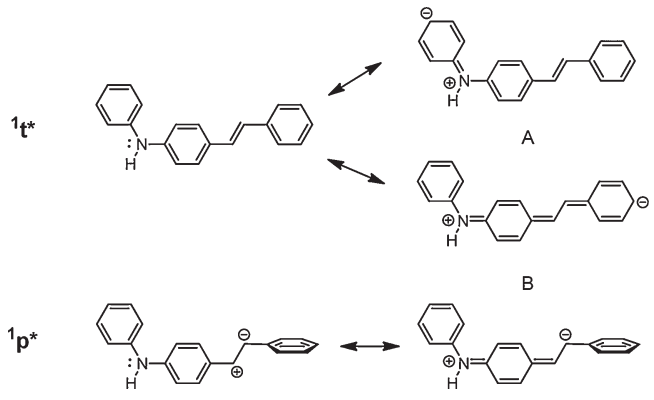

Scheme 1. Resonance structures of the $^1t^*$ and $^1p^*$ states of **p1H**.

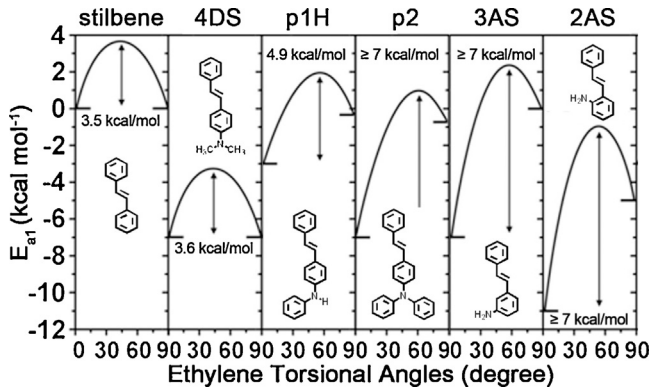

Fig. 9. The relative energies of the $^1t^*$ and $^1p^*$ states and the C=C torsion barriers for a series of *trans*-aminostilbenes relative to the parent *trans*-stilbene.

Introducing a second *N*-phenyl group to **p1H** (i.e., *trans*-4-(*N*,*N*-diphenylamino) stilbene **p2**, Chart 3) further enhances the Φ_f from 0.51 to 0.62 in hexane and from 0.34 to 0.95 in MeCN [57]. By following the above concept of resonance stabilization effect on $^1t^*$ and $^1p^*$, the second *N*-phenyl group is expected to further enlarge the energy difference between the $^1t^*$ and the $^1p^*$ states and thus further increase the C=C torsion barrier (Fig. 9). Consequently, the singlet-state C=C torsion is rather inefficient for **p2**, and the observed *trans* → *cis* isomerization is mainly via the triplet excited state. That fluorescence and the C=C torsion determines the deactivation of photoexcited **p2** is evidenced by the observation of $\Phi_f + 2\Phi_{tc} \approx 1.0$ in both nonpolar and polar solvents. However, unlike **p1H** that possesses a lower Φ_f in more polar solvents, the opposite is true for **p2**. The difference in solvent effect might result from the singlet vs. triplet mechanism of the C=C torsion for **p1H** and **p2**, respectively. For **p1H**, increasing the solvent polarity lowers the singlet-state C=C torsion barrier and thus reduces the Φ_f. In the case of **p2**, increasing the solvent polarity decreases the rate for the $^1t^* \rightarrow {}^3t^*$ intersystem crossing and thus increases the Φ_f.

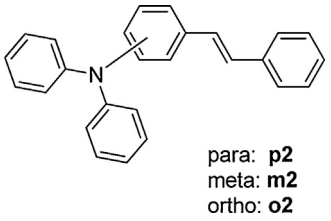

Chart 3. Structures of *trans*-2-, -3-, and -4-(*N*,*N*-diphenylamino)stilbenes.

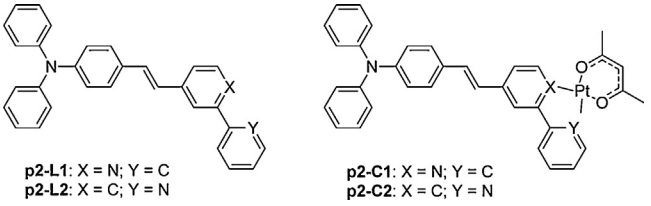

Chart 4. Structures of C^N ligands and Pt complexes derived from *trans*-4-(*N*,*N*-diphenylamino)stilbene.

It should be noted that the *N*-arylamino conjugation effect on raising the C=C torsion barrier in favor of fluorescence is a phenomenon of the S_1 but not the T_1 chemistry. This was demonstrated with the **p2**-derived C^N ligands **p2-L1** and **p2-L2** and their Pt complexes **p2–C1** and **p2–C2** (Chart 4) [58]. While both C^N ligands conform to $\Phi_f + 2\Phi_{tc} \approx 1.0$ with high Φ_f (0.68–0.95) and low Φ_{tc} (0.02–0.25) in both nonpolar and polar solvents, the Pt complexes are of extremely weak fluorescence and phosphorescence ($\Phi < 0.001$) with the Φ_{tc} values close to 0.50 in degassed solutions at ambient temperatures. Since the photochemistry of the Pt complexes is dominated by the triplet excited states as a result of efficient intersystem crossing induced by the heavy atom Pt, the fact of $2\Phi_{tc} \approx 1.0$ indicates that the decay of T_1 is dominated by the C=C torsion, a feature also known for *trans*-stilbenes. A diminishment of Φ_{tc} by 34% was observed for **p2–C2** in aerated dichloromethane solutions owing to quenching of the T_1 state by molecular oxygen [58].

4.2. The meta-amino and para, para-diamino effects

Besides the *N*-arylamino conjugation effect, two other amino substituent effects that significantly raises the C=C torsion barrier in favor of fluorescence are the *meta*-amino and *para,para*-diamino effects [59,60]. This is illustrated by the comparison of *trans*-3-aminostilbene (3AS) [54], *trans*-4-aminostilbene (4AS) [54], and *trans*-4,4′-bis(dimethylamino) stilbene (4DDS) [61,62] in cyclohexane or hexane (Chart 5), which possess a Φ_f of 0.78, 0.05, and 0.81, respectively.

By following the same concept for the interpretation of the *N*-arylamino conjugation effect, both the *meta*-amino and the *para, para*-diamino substituents lower the $^1t^*$ state more than the $^1p^*$ state such that the C=C torsion barrier is increased (Fig. 9). The stabilization of the $^1t^*$ state by the *meta*-amino substituent is a consequence of the photoinduced amino → stilbene ICT behavior, as evidenced by the red-shifted ICT absorption band and by the high solvatofluorochromicity. However, for the zwitterionic or diradical $^1p^*$ state little or no resonance stabilization could be

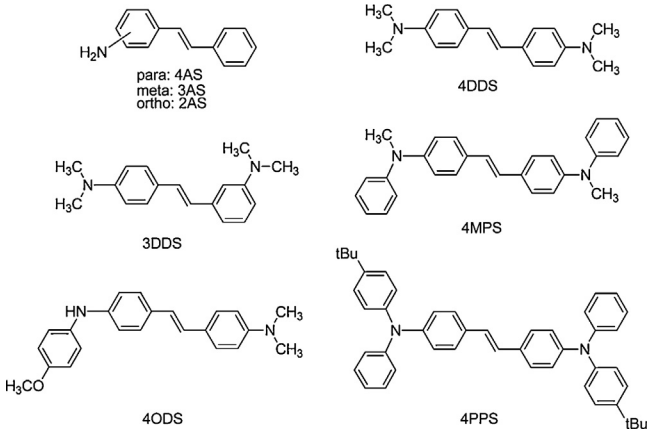

Chart 5. Structures of *trans*-aminostilbenes and *trans*-diaminostilbenes.

exerted by the *meta*-amino group. In the case of the *para,para*-diamino systems, the stabilization of the $^1t^*$ state by both amino groups is evidenced by the red-shifted absorption and fluorescence maxima of 4DDS vs. 4DS [63]. The absence of a similar extent of stabilization to the $^1p^*$ state by the second amino group in 4DDS appears to indicate that the $^1p^*$ state possess a zwitterionic character, in which the negative charge was not favored by the electron-donating amino group.

The *meta*-amino effect on raising the C=C torsion barrier is even more pronounced than the *para*-*N*-arylamino conjugation effect. The barrier for 3AS was estimated to be larger than 7 kcal/mol (Fig. 9), which renders the singlet-state C=C torsion rather inefficient as compared with the fluorescence and the $S_1 \rightarrow T_1$ intersystem crossing. Therefore, the *trans* → *cis* isomerization occurred mainly in the triplet excited state.

Although both 3AS and 4AS possess an ICT character for the $^1t^*$ state, the degree of charge separation and thus the excited-state dipole moment is different, which is larger for the meta isomer. This can be readily understood by the weaker electronic couplings between the D and A groups in the *meta* vs. *para* system, as evidenced by the lower intensity of the ICT absorption band. The weak D–A electronic coupling in *meta*-amino systems is sufficient to induce ICT from D to A upon photoexcitation, but once charge separation has occurred the charge delocalization and recombination in the relaxed PICT state becomes inefficient, leading to large dipole moments and low fluorescence rate for the PICT state. This explains not only the longer wavelength of fluorescence maximum (446 vs. 423 nm) but also the longer fluorescence lifetime (11.7 vs. ~0.1 ns) for 3AS vs. 4AS in acetonitrile [54]. Note that the excited state deactivation is a game of kinetics: the relatively higher is the rate for a specific decay channel than all the other pathways, the larger is the quantum efficiency for that channel, regardless the absolute value of the rate constants. In other words, the low fluorescence decay rates for *meta*-amino systems do not hamper the character of high fluorescence quantum yields, because the competing nonradiative reactions of the C=C torsion and $S_1 \rightarrow T_1$ intersystem crossing are of even lower rates.

5. Marriage of the *meta*-amino, *para*-*N*-arylamino, and *para, para*-diamino effects

What is the outcome for a stilbene system that combines the *N*-arylamino and *meta*-amino effects (i.e., *meta*-*N*-arylamino substitutions)? This question can be answered by the systems **m1*R*** (***R*** = H, Me, OM, and CN, Chart 2) and **m2** (Chart 3), in which the *meta*-amino group is substituted with one or two *N*-aryl groups. The discussion could be divided into two different conditions, i.e., TICT-free vs. TICT-forming conditions. According to the above-mentioned criteria for the nature of ICT states, **m1H**, **m1CN**, and **m2** are TICT-free fluorophores, but **m1Me** and **m1OM** belong to TICT-forming species [64,65].

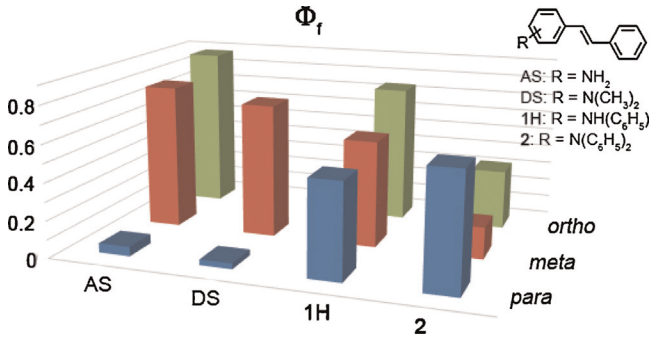

Fig. 10. Comparison of Φ_f of the positional isomers of AS, DS, **1H**, and **2** in hexane or cyclohexane.

The relative Φ_f of 3AS, 3DS, **m1H**, and **m2** in cyclohexane is depicted in Fig. 10. For comparison, the Φ_f values of 4AS, 4DS, **p1H**, and **p2** in hexane are included. Obviously, the marriage of the two fluorescence-enhancing *meta*-amino and *N*-arylamino conjugation effects on stilbene did not further promote the fluorescence quantum efficiency. Instead, it led to a decrease of Φ_f relative to either one of the parent aminostilbenes. For example, **m2** results from a marriage of **p2** and 3AS; the Φ_f of **m2** is lower than **p2** and 3AS in both hexane (0.17, 0.62, and 0.78, respectively) and acetonitrile (0.14, 0.95, and 0.55, respectively). The Φ_f diminishment results from a decrease of the rate constants for fluorescence and from an increase of the rate constants for the $S_1 \rightarrow T_1$ process. We reasoned that the *N*-aryl groups lower the energy level of the weakly allowed S_1 state of 3AS such that the S_1–S_2 energetic gap is increased but the S_1–T_1 gap is decreased. Since the π,π^*-based $S_0 \rightarrow S_2$ transition is more allowed than the ICT-based $S_0 \rightarrow S_1$ transition for the meta systems, increasing the S_1–S_2 energetic gap would reduce intensity borrowing of the S_1 state from the S_2 state and thus reduce the rate for fluorescence. In addition, decreasing the S_1–T_1 gap would facilitate the intersystem crossing process to form the T_1 state, which is deactivated mainly via the C=C torsion (vide supra).

Regarding the TICT-forming activity, the increased charge separation for the *meta* vs. *para* systems in the S_1 (PICT) state might facilitate the formation of a TICT state by twisting the stilbene-amino C—N bond. This is indeed demonstrated by the difference between **m1Me** and **p1Me**: namely, **p1Me** belongs to the TICT-free category (vide supra), but **m1Me** is able to form a TICT state by twisting the stilbene-amino C—N bond in acetonitrile ($\Phi_f + 2\Phi_{tc} \approx 0.58$).

On the other hand, the character of decreased charge delocalization between the amino and stilbene groups for the *meta* vs. *para* systems in the S_1 state imposes an opposite influence in the TICT-forming activity of **1CN**: namely, unlike the TICT-forming **p1CN**, **m1CN** does not undergo TICT state formation. The lack of TICT-forming activity for **m1CN** is associated with the inefficient charge translocation across the stilbene-amino C—N bond (Fig. 5). More specifically, the polarization direction of the Franck–Condon ICT or PICT state is from the amino (D) to the stilbene (A), which is independent of the nature of the *N*-substituents and the position of the amino group on stilbene. However, the polarization direction of the TICT state of **1CN** is from the amino (D) to the benzonitrile (A) group. Consequently, formation of the TICT state from either the Franck–Condon ICT or the PICT state requires charge translocation by converting the role of the stilbene group from A to D during the twisting the benzonitrile–aminostilbene C—N bond. As discussed above, charge translocation (delocalization) through the amino nitrogen atom is effective in the para system but not in the meta system, which determines the fate of the torsional relaxation of **p1CN** and **m1CN**.

Regarding the outcome of a marriage of the *meta*-amino and the *para,para*-diamino effect, the comparison of 4DDS and its *meta*-*para* isomer 3DDS offers a clue to this issue. The excited state of 3DDS is governed mainly by the *para*-amino rather than the *meta*-amino group such that the Φ_f in hexane or methylcyclohexane is in the order 4DDS (0.81) > 3DS (0.72) > 3DDS (0.33) > 4DS (0.03) [66]. Since no TICT states could be formed by these systems (i.e., $\Phi_f + 2\Phi_{tc} \approx 1.0$ in both nonpolar and polar solvents), the opposite order is true for their relative Φ_{tc} values.

Furthermore, the marriage of the *para,para*-diamino and *N*-arylamino effects also led to a decrease of Φ_f, as illustrated with 4MPS (0.73 in THF) and 4PPS (0.45 in THF) relative to 4DDS (Chart 5) [67]. In the case of *N*-(4-methoxyphenyl) amino derivative 4ODS, the TICT-forming activity in acetonitrile is not

inhibited but largely diminished ($\Phi_f + 2\Phi_{tc} = 0.57$) by the presence of a dimethylamino group, consistent with the decreased push–pull character of this system as compared with **p1OM** [62].

In summary, all the marriages of either two of the three fluorescence-enhancing amino substituent effects lead to a negative outcome.

6. The ortho-amino effect

The distinct quantum efficiencies in fluorescence, the C=C torsion, and the TICT state formation between the *meta*- and *para*-aminostilbenes triggers the investigation of the corresponding ortho systems 2AS (*trans*-2-aminostilbene), **o1*R*** (***R*** = H, Me, OM, and CN, Chart 2), and **o2** (Chart 3) to gain a complete picture on the amino-position effect [57]. The results show that the *ortho* systems resemble the corresponding *meta* systems more than the *para* counterparts. In brief, the ortho systems possess a high Φ_f value in nonpolar solvents as a result of a high C=C torsion barrier in S_1, undergo the C=C torsion mainly in T_1, and form a TICT state in polar solvents for the cases of **o1Me** and **o1OM** but not for 2AS, **o1H**, **o1CN**, and **o2**. The similarity in the excited-state behavior for the *ortho*- and the *meta*-amiostilbenes is reminiscent of the *ortho*–*meta* effect termed by Howard Zimmerman in 1970s from the observations of a similar photochemical activity for meta and ortho derivatives as compared with their para counterparts [68].

To account for the high C=C torsion barrier, the *o*-amino substituents should stabilize the $^1t^*$ state more than the $^1p^*$ state. Stabilization of the $^1t^*$ state could be attributed to extensive configuration interactions between the ICT state and the locally excited (LE) states owing to decreased molecular symmetry and planarity. The steric interactions between the amino and the stilbene groups account for the decreased planarity of the ortho systems. According to the absorption spectra of 2AS, 3AS, and 4AS, the degree of stabilization of the $^1t^*$ state by the amino group is in the order 2AS > 3AS ≈ 4AS [54]. However, the resonance stabilization of $^1p^*$ state by the amino group is expected to be in the order 4AS > 2AS > 3AS, because the decreased planarity of the anilino group in 2AS vs. 4AS would reduce the resonance stabilization interactions. Consequently, the C=C torsion barrier would be 2AS ≈ 3AS > 4AS. The *ortho* systems also resemble the meta systems by having long fluorescence lifetimes. In particular, **o2** displays an unprecedented long fluorescence lifetime for unconstrained *trans*-stilbenes (24.5 ns) in solutions at ambient temperature [57].

The lack of TICT activity for **o1CN** in acetonitrile deserves a comment. In the model that explains the different TICT-forming activity of **p1CN** vs. **m1CN** (Fig. 5), the efficiency of charge translocation plays an important role in driving the Franck–Condon ICT or PICT state toward the TICT state. Since the *ortho*–*para* quinoidal resonance structures predict an efficient charge translocation for **o1CN** as well as for **p1CN**, the lack of TICT-forming activity for **o1CN** should be attributed to other reasons. One possible reason is the steric effect of the *o*-amino group that reduces the stability of the quinoidal resonance form and thus the charge translocation efficiency. Another possible origin is the relatively lower energy of the PICT state in **o1CN** vs. **p1CN**, which might energetically disfavor the PICT → TICT conversion.

7. Steric effects on TICT-forming activity

The *ortho*-amino effect reveals the important role of steric hindrance and structural planarity in the excited-state behavior of *trans*-aminostilbenes. To gain further insights into the ground-state steric effects on the interplay among the fluorescence, C=C torsion, and TICT-forming activity of *trans*-aminostilbenes, a series of methyl-substituted **p1CN** derivatives having different degree of twisting in the stilbene moiety were investigated (Chart 6) [56].

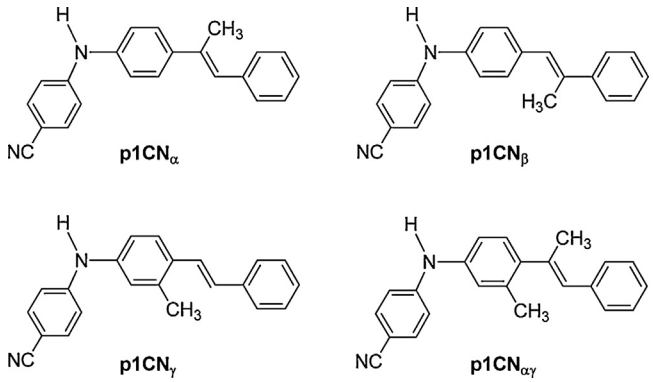

Chart 6. Structures of methyl-substituted *trans*-4-(*N*-(4-cyanophenyl)amino)stilbenes.

The methyl group is located at the vinylene α-(**p1CN$_\alpha$**) or β-carbon (**p1CN$_\beta$**) position or at the amino-substituted phenylene ring (**p1CN$_\gamma$**). The dimethyl-substituted system **p1CN$_{\alpha\gamma}$** was also investigated. According to the X-ray crystal structures and AM1 calculations, the relative molecular planarity of the stilbene group in these aminostilbenes is in the order **p1CN**–**p1CN$_\gamma$** > **p1CN$_\alpha$**–**p1CN$_\beta$** > **p1CN$_{\alpha\gamma}$**.

The reduced stilbene planarity in **p1CN$_\alpha$**, **p1CN$_\beta$**, and **p1CN$_{\alpha\gamma}$** relative to **p1CN** imposes a significant impact on the fluorescence profile: whereas the fluorescence spectra of **p1CN** and **p1CN$_\gamma$** show vibrational structures in hexane and PICT–TICT dual bands in acetonitrile, the spectra become structureless in hexane and show a single broad TICT emission band in acetonitrile for **p1CN$_\alpha$**, **p1CN$_\beta$**, and **p1CN$_{\alpha\gamma}$** (Fig. 11). In conjunction with the reduced Φ_f and increased Φ_{tc}, it was concluded that ground-state twisting of the stilbene moiety facilitates the deactivation of the PICT state via the C=C torsion, particularly in polar solvents, such that the quantum efficiency of the TICT state formation is also diminished. The observed steric effect results from a dramatic decrease of the singlet-state C=C torsion barrier. For comparison, the barrier was determined to be >7.4 kcal/mol for **p1CN** in methylcyclohexane, but it is ~3.3 kcal/mol for **p1CN$_\beta$** under the same condition [56].

Regarding the effect of stilbene planarity on the TICT-forming activity, the influence is small when the stilbene planarity is modestly reduced as in the case of **p1CN$_\alpha$** and **p1CN$_\beta$**; however, for the largely twisted system such as **p1CN$_{\alpha\gamma}$**, the C—N bond torsion efficiency is increased because of localized excitation at the

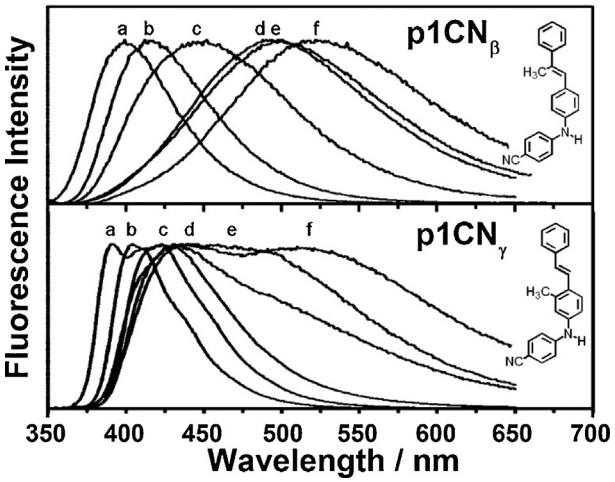

Fig. 11. Normalized fluorescence spectra of **p1CNβ**, and **p1CN$_\gamma$** in (a) hexane, (b) toluene, (c) THF, (d) dichloromethane, (e) acetone, and (f) acetonitrile. Modified from reference [56].

cyanodiphenylamine moiety. The Φ_{TICT} value, as calculated by the equation: $\Phi_{TICT} = 1 - (\Phi_f + 2\Phi_{tc})$, is in the order **p1CN** (0.9)–**p1CN$_{\alpha\gamma}$** (0.9) > **p1CN$_{\beta}$** (0.8) > **p1CN$_{\alpha}$** (0.6).

8. Strong push–pull *trans*-aminostilbenes

In principle, increasing the push–pull strength of a D–A system by increasing either the electron-donating ability of the D group or the electron-accepting strength of the A moiety would enhance the propensity of the TICT state formation because of an increased extent of charge separation in the Franck–Condon ICT state. A good example for the former case is illustrated by the series of **p1*R*** on going from the TICT-free **p1H** and **p1Me** to the TICT-forming **p1OM**, in which the electron-donating ability of the *N*-arylamino (D) group is in the order **p1H** < **p1Me** < **p1OM** [51]. The high TICT-forming activity of **p1OM** shows that the *N*-(4-methoxyphenyl) amino donor is sufficiently strong to drive the formation of a TICT state even when the stilbene is not substituted with an electron-withdrawing group.

A good example for illustrating the relationship between the electron-accepting strength of the A moiety and the TICT-forming activity of *trans*-aminostilbenes comes from the cyano- and nitro-substituted systems **p3*R*** (***R*** = H, Me, OM, and CN, Chart 7), **p4MP**, 4DCS, and 4DNS [52]. The cyano substituent in **p3*R*** does enhance the TICT-forming propensity as compared to the parent systems **p1*R***. For example, **p1Me** has negligible TICT-forming propensity, but the Φ_{TICT} for **p3Me** in acetonitrile was estimated to be as large as ~0.8. The cyano effect is also noticeable in the TICT-active **p1OM** system, as **p3OM** display a larger and nearly quantitative yield for forming the TICT state ($\Phi_{TICT} > 0.97$). The TICT state of **p3OM** is essentially non-fluorescent, as evidenced by the much smaller half-bandwidth (~4900 cm^{-1}) for **p3OM** relative to that for **p1OM** (~6200 cm^{-1}) in acetonitrile and by the opposite temperature effect on the fluorescence intensity of **p3OM** vs. **p1OM** (vide supra) [52]. The decreased fluorescing ability for **p3OM** vs. **p1OM** might be associated with the larger driving force toward the TICT state. On the other hand, the cyano effect in 4DCS and **p3H** is insufficient to induce the formation of a TICT state with the *N*-phenylamino or *N,N*-dimethylamino donor. The dicyano system **p3CN** is also TICT silent, in contrast to the TICT-forming **p1CN**. Evidently, the A–D–A configuration in **p3CN** does not favor the TICT states from torsion of either one of the two D–A bonds.

Nitro-substituted aminostilbenes remark a different story about the TICT state of D–A systems. It is long-term recognized

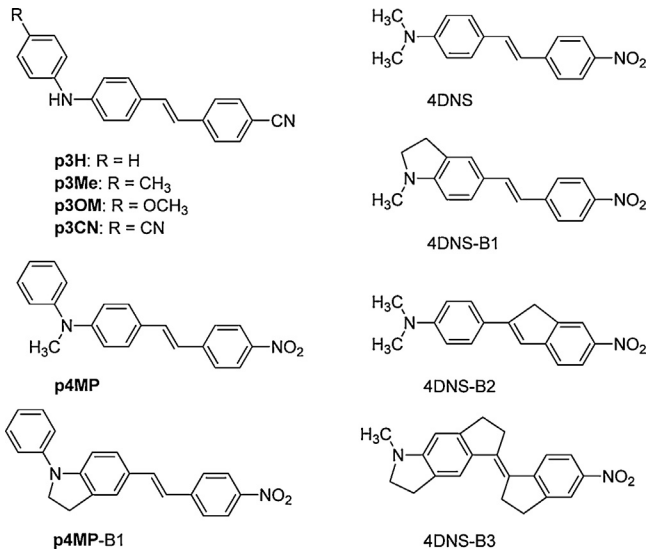

Chart 7. Structures of strong push–pull *trans*-4-aminostilbenes.

that 4DNS displays low quantum efficiencies for fluorescence and *trans* → *cis* isomerization in solvents of medium and strong polarity, and the argument of TICT state formation fits very well with the TICT parameter $\Phi_f + 2\Phi_{tc} << 1.0$ [69]. However, identification of the bond that twists with the ring-bridged systems 4DNS-B1 [69] and 4DNS-B2 [70] (Chart 7) has failed, because both of them also follow the same behavior of $\Phi_f + 2\Phi_{tc} << 1.0$ as the parent 4DNS system in polar solvents. Similar phenomena were also observed for **p4MP** and its ring-bridged derivative **p4MP**-B1. Two possible scenarios might account for these observations: first, more than one type of TICT states could be formed, and thus constraining one of the single bonds could not completely inhibit the TICT state formation; alternatively, there is only one type of TICT state, but the bond that twists is neither the stilbene-amino C—N bond nor the nitrophenylene–vinylene C—C bond. As the arene-nitro C—N bond has been inferred to be responsible for the excited-state deactivation of many nitroaromatics [71–74], we designed the multisite constrained 4DNS model system 4DNS-B3 to investigate whether the NO_2-twisting is a viable candidate for the TICT state of 4DNS [75].

The limited torsional freedom of 4DNS-B3, only about the stilbene-nitro C—N and the central C=C bonds, allows one to conclusively address the structural nature of the TICT state of 4DNS. Like 4DNS, 4DNS-B3 displays the behavior of $\Phi_f + 2\Phi_{tc} \approx 1.0$ in hexane but not in tetrahydrofuran (THF) or more polar solvents, revealing that the NO_2 twisting is an effective channel to deactivate the PICT state. The absence of spectral broadening in THF vs. hexane and the single exponential decay times observed for 4DNS-B3 show that the NO_2 twisting does not lead to an emissive TICT state. This is reminiscent of **p3OM** and appears to say that the TICT state of strong push–pull *trans*-aminostilbenes tends to be nonfluorescent.

TDDFT calculations on 4DNS-B3 in dichloromethane provide the structural and energetic details for the TICT formation and deactivation processes (Fig. 12). Structural relaxation of the Franck–Condon ICT state first involves with the planarization of the amino N atom, in which the pyramidal geometry with a wagging angle of ~20° is reduced to 5°, followed by the NO_2 twisting and the pyramidalization of the nitro N atom (wagging angle is ~18°). The driving forces for the first and the second steps

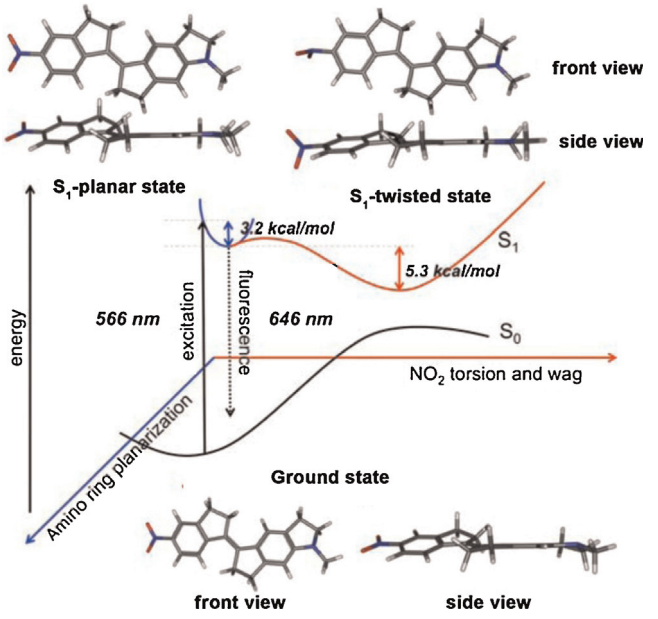

Fig. 12. Simplified scheme for the potential energy surfaces along the nitro torsion/wag and the amino planarization coordinates for the singlet excited state of 4DNS-B3 in CH_2Cl_2. Modified from Ref. [74].

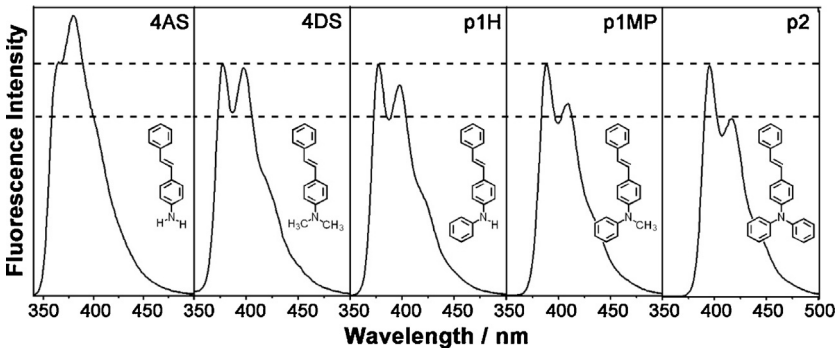

Fig. 13. Fluorescence spectra of 4AS, 4DS, **p1H**,**p1MP**, and **p2** in hexane. The spectra were normalized with respect to the 0,0 band. Modified from [55].

of structural changes are ~3.2 and ~5.3 kcal/mol, respectively. The small S_0–S_1 energy gap (8.5 kcal/mol) for the TICT geometry accounts for the ultrafast internal conversion and thus the lack of emission of the TICT state.

9. Geometry of the amino groups in trans-aminostilbenes

The planarization (i.e., sp^2 hybridization) of the amino N atom of *trans*-aminostilbenes on going from the Franck–Condon ICT state to the PICT (S_1) state affects not only the fluorescence maxima but also the fluorescence vibrational structures in nonpolar solvents. This was illustrated with the series of the *N*-methyl and *N*-phenyl substituted para systems 4AS, 4DS, **p1H**, **p1MP** (*trans*-4-*N*-methyl-*N*-phenylaminostilbene) and **p2** in hexane, in which the intensity ratio of the fluorescence 0–1 vs. the 0–0 band, corresponding to the Huang–Rhys factor (S) [76] gradually decreases along the series (i.e., 4AS > 4DS > **p1H** > **p1MP** > **p2**, Fig. 13). The Huang–Rhys factor qualitatively describes the extent of changes in equilibrium displacement of related vibrations. The vibrational spacing is $1300 \pm 80\ cm^{-1}$, which is similar to those of *trans*-stilbene and is associated with several vibrational modes, including C—Ph stretching and torsion, ethenyl C=C stretching and in-plane bending, and phenyl C—C stretching. However, the major structural difference along the compound series is the planarity of the amino group. A simple parameter to describe the amino geometry is the sum of the three bond angles (θ) about the N atom. AM1-calculations show that the θ values are in the order **p2** (360.0°) > **p1MP** (357.3°) > **P1H** (353.9°) > 4DS (351.6°) > 4AS (342.9°), revealing that the more the *N*-methyl or *N*-phenyl substituents are in the system, the more planar is the geometry of the amino N atom in the ground state. The fact that increasing the θ values is accompanied with a decrease of the *S* values is consistent with the fluorescing state being a PICT state, because the degree of structural relaxation from the Franck–Condon excited state to the PICT state is of smaller extent with the more planar amino group. The correlation between θ and *S* also indicates a strong coupling of the C—N stretching with the stilbene vibrational modes.

10. Applications of *trans*-aminostilbenes

As mentioned at the beginning, *trans*-aminostilbenes have found applications as fluorescent probes, cell imaging dyes, and the active materials in a variety of optoelectronic devices. We have adopted the fluorescence-enhancing *N*-arylamino conjugation effect and the TICT-forming *N*-(4-methoxyphenyl) amino substituent effect to design fluoroionophores of intriguing fluorescence signaling mechanisms.

The fluoroionophore **5** (Chart 8) was designed to interact with transition metal ions via the dipyridalamino (dpa) group, and **5** was expected to be strongly fluorescent because of its structural analogy to **p2**. Indeed, the Φ_f of **5** in acetonitrile is as high as 0.57 and it undergoes an on-off fluorescence response to the addition of one equivalence of Zn(II) and Pb(II) ions [77,78]. The fluorescence quenching is associated with an orthogonal twist of the stilbene–dpa C—N bond upon binding with the metal ions, as shown by the X-ary crystal structures of the complex **5**·$ZnCl_2$. In conjunction with the corresponding behavior of the related systems **6** and **7**, we were able to conclude that the fluorescence quenching results from photoinduced electron transfer (PET) from the stilbene to the deconjugated dpa–Zn(II) moiety in the complex. In other words, the dpa group functions as an electron donor in **5**

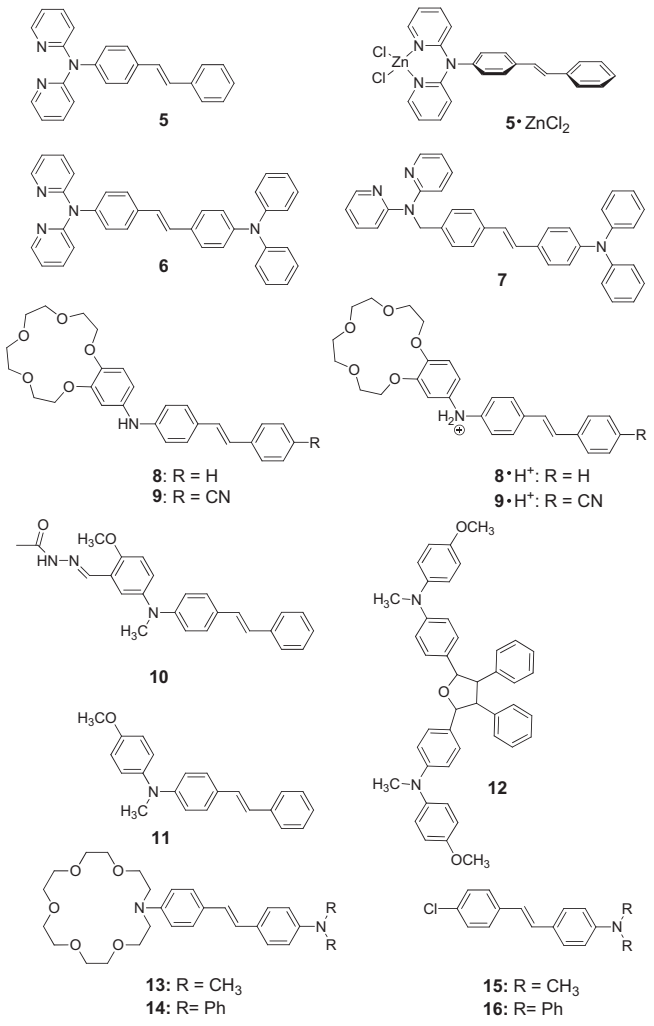

Chart 8. Structures of fluorescent probes derived from *trans*-4-aminostilbenes.

but as an electron acceptor in **5**·$ZnCl_2$ owing to the coordination with metal ions.

Fluoroionophores **8** and **9** (Chart 8) were designed by incorporating the benzocrown ionophore to the TICT-forming **p1OM** and **p3OM** for interacting with alkaline metal ions Mg(II) and Ca(II) [5]. When the probes are in the neutral form, the ion recognition induces a fluorescence turn-on signal as a result of the deactivation of the TICT-forming pathway. Note that the majority of fluorescence turn-on probes rely on perturbation of a PET process in a donor-σ linker-acceptor configuration. The TICT mechanism demonstrated by **8** and **9** provides an alternative methodology for fluorescence turn-on probes. When the probes are protonated at the amino N atom under highly acidic conditions (**8**·H^+ and **9**·H^+), a localized emission from the *trans*-stilbene moiety is responsible for the optical transition of the photoexcited probes. The ion binding restores the PICT fluorescence by expelling the ammonium proton and leads to dual fluorescence that allows ratiometric detection. This case demonstrates the potential applications of TICT-forming *trans*-aminostilbenes as sensory materials.

Another example of TICT-forming *trans*-aminostilbenes as fluorescence turn-on probes is illustrated by **p1OM** and its acetylhydrazone derivative **10** (Chart 9) for the detection of Cu (II) [6]. Although the phenomenon of fluorescence turn-on in response to Cu(II) was observed, the mechanism was not simply from binding-induced deactivation of the TICT-forming channel. Instead, a redox reaction occurs between the probe molecule (reductant) and Cu(II) (oxidant) and the product is of stronger fluorescence than the probe molecule. This was demonstrated with **11**, which does not have the Cu(II) ionophore but performs the same spectroscopic behavior as **10**, indicating that Cu(II) binding is not required for turning on the fluorescence. The redox product has been attributed to a tetrahydrofuran derivative (**12**) formed by the dimerization of the radical cation intermediates and the involvement of one molecule of water. A dramatic blue shift of fluorescence (~170 nm) is consistent with the decrease of the π-conjugation length in the redox product.

We also employed the azacrown-derived *para,para*-diaminostilbenes **13** and **14** (Chart 8) for the investigation of the supramolecular interactions between the azacrown group and Ca(II). An interesting correlation was found for the electronic absorption and emission spectra of **13**·$Ca(ClO_4)_2$ and **14**·$Ca(ClO_4)_2$ and the corresponding chloro-substituted *trans*-aminostilbenes **15** and **16** in acetonitrile, indicating that the electron-donating azacrown group becomes an electron-withdrawing group that resembles a Cl atom upon binding with Ca(II). Regarding the fact that N and Cl have similar electronegativity but the lone-pair electrons of N have larger electron-donating ability than those of Cl to the stilbene moiety, the correlation indicates that Ca(II) hamper the interactions of the N lone-pair with the stilbene moiety either by twisting away from the stilbene plane or by pyramidalizing the N geometry to an extent that the overall electronic character of the azacrown N resembles that of a Cl atom [79].

The fluorescence-enhancing *meta*-amino and *N*-arylamino conjugation effects observed for *trans*-aminostilbenes could also apply to other chromophores. This has been demonstrated with the green fluorescence protein (GFP) chromophore, 4-hydroxybenzylidenedimethylimidazolinone (*p*-HBDI), by replacing the *para*-OH group with *para*-*N*-arylamino or *meta*-amino groups (Chart 9) [80,81]. Unlike the strong fluorescence of GFP ($\Phi_f \sim 0.8$), the chromophore *p*-HBDI is nearly nonfluorescent ($\Phi_f < 0.001$) in bulk solutions at ambient temperatures as a result of ultrafast exocyclic C=C (i.e., the Z → E isomerization) and/or C—C rotation (i.e., a TICT state formation). The *para*-amino analog *p*-ABDI resembles *p*-HBDI with negligible fluorescence. However, the *meta*-amino isomer *m*-ABDI displays unprecedentedly high fluorescence quantum yield of 0.34 in hexane, which is more than 340 times larger than the para isomer. Such a *meta*-amino effect on fluorescence enhancement is much more significant than the case of *trans*-aminostilbenes. In the case of *N*-arylamino systems such as **17** and **18**, fluorescence enhancement ($\Phi_f = 0.001–0.056$) was also observed, albeit to a smaller extent. Since the relationship $\Phi_f + 2\Phi_{ZE} \approx 1.0$ holds for *p*-HBDI, *p*-ABDI, *m*-ABDI, **17**, and **18** in acetonitrile [80], the TICT-forming pathway either by twisting the exocyclic C—C or C—N bond should be rather unimportant in their excited-state deactivation. This has provided a new approach in resolving the controversy of the C=C vs. C—C torsion in accounting for the fluorescence quenching of *p*-HBDI [80].

Besides the fluorescence-enhancing substituent effects, the TICT-forming amino substituent *para*-*N*-(4-methoxyphenyl) amino in *trans*-aminostilbenes could also induce the TICT state formation for the GFP-like chromophores, as evidenced by **19** and the ring-bridged system **20**. Whereas **19** displays $\Phi_f + 2\Phi_{ZE} \approx 1.0$ in hexane but not in THF and acetonitrile, the relationship $\Phi_f + 2\Phi_{ZE} \approx 1.0$ holds for **20** in all three solvents. The corresponding Φ_f values for **19** and **20** are 0.003 and 0.016 in THF and <0.001 and 0.025 in acetonitrile, respectively, showing the same solvent polarity dependent TICT-forming activity observed for *trans*-aminostilbenes.

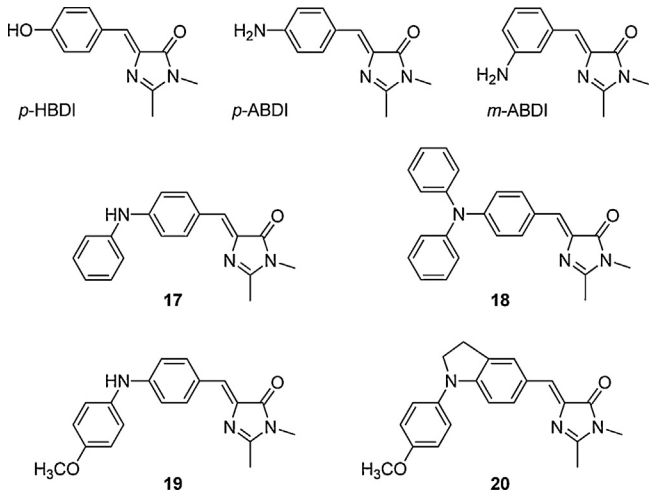

Chart 9. Structures of GFP chromophore and its amino analogs.

11. Summary and perspectives

Three pathways, fluorescence, the C=C torsion, and formation of a TICT state, account for the deactivation of photoexcited *trans*-aminostilbenes in dilute solutions at ambient temperature. Table 1 summarizes the quantum yield data Φ_f, Φ_{tc}, and Φ_{TICT} (i.e., $1 - (\Phi_f + 2\Phi_{tc})$) of the typical *trans*-aminostilbenes discussed in this feature article. The relative quantum efficiency of these pathways strongly depends on the nature and position of the amino group, the solvent polarity, and the substituents having significant steric or electronic impacts. This provides a good opportunity toward the design of novel photoactive materials based on *trans*-aminostilbenes and related systems. For example, to have high Φ_f values, *meta*-amino, *para*-*N*-arylamino, and *para,para*-diamino systems are promising candidates. To have high TICT-forming efficiency (i.e., low Φ_f and Φ_{tc} values), the use of *N*-(4-methoxyphenyl) amino or nitro group is effective but polar solvents are required. For the rest of systems, the C=C torsion that corresponds to the *trans* → *cis* isomerization would dominate the excited state behavior of *trans*-aminostilbenes, as is the case of the parent *trans*-stilbene. The C=C torsion generally occurs in the singlet

Table 1
Data of quantum yields for fluorescence (Φ_f), *trans* → *cis* isomerization (Φ_{tc}), and formation of a TICT state (Φ_{TICT}) of *trans*-aminostilbenes.

Compd.	Solvent	Φ_f	Φ_{tc}	$\Phi_f + 2\Phi_{tc}$	Φ_{TICT}	Ref.
p1H	*n*-Hexane	0.51	0.24	0.99		[51]
	THF	0.42	0.24	0.90		[51]
	CH_2Cl_2	0.38	0.34	1.06		[51]
	MeCN	0.34				[51]
p1Me	*n*-Hexane	0.53				[51]
	THF	0.55	0.28	1.11		[51]
	CH_2Cl_2	0.49	0.28	1.05		[51]
	MeCN	0.41				[51]
p1Cl	*n*-Hexane	0.58				[51]
	THF	0.53	0.27	1.07		[51]
	CH_2Cl_2	0.48	0.29	1.06		[51]
	MeCN	0.43				[51]
p1CF	*n*-Hexane	0.68				[51]
	THF	0.49	0.18	0.94		[51]
	CH_2Cl_2	0.43	0.22	0.87		[51]
	MeCN	0.25				[51]
p1CO	*n*-Hexane	0.72				[51]
	THF	0.38	0.11	0.60	0.40	[51]
	CH_2Cl_2	0.03	0.04	0.11	0.89	[51]
	MeCN	0.004				[51]
p1OM	*n*-Hexane	0.60	0.10	0.80		[51]
	THF	0.36	0.05	0.46	0.54	[51]
	CH_2Cl_2	0.24	0.09	0.42	0.58	[51]
	MeCN	0.007				[51]
p1OM-B1	*n*-Hexane	0.81				[51]
	MeCN	<0.001				[51]
p1OM-B2	*n*-Hexane	0.75				[51]
	CH_2Cl_2	0.66	0.25	1.16		[51]
	MeCN	0.68				[51]
p1CN	*n*-Hexane	0.75	0.16	1.07		[51]
	THF	0.46	0.16	0.78	0.22	[51]
	CH_2Cl_2	0.11	0.14	0.39	0.61	[51]
	MeCN	0.015				[51]
p1CN-B1	*n*-Hexane	0.81				[51]
	CH_2Cl_2	0.02				[51]
	MeCN	0.81				[51]
p1CN-B2	*n*-Hexane	0.78				[51]
	MeCN	0.014				[51]
p1CN-B3	*n*-Hexane	0.32	0.30	0.93		[56]
	MeCN	0.01	0.02	0.05	0.95	[56]
p1CN$_\alpha$	*n*-Hexane	0.004	0.48	0.96		[56]
	THF	0.018	0.43	0.88	0.12	[56]
	MeCN	0.02	0.22	0.46	0.54	[56]
p1CN$_\beta$	*n*-Hexane	0.07	0.45	0.97		[56]
	THF	0.12	0.31	0.74	0.26	[56]
	MeCN	0.021	0.11	0.24	0.76	[56]
p1CN$_\gamma$	*n*-Hexane	0.71	0.15	1.01		[56]
	THF	0.52	0.16	0.84	0.16	[56]
	MeCN	0.025	0.06	0.15	0.85	[56]
p1CN$_{\alpha\gamma}$	*n*-Hexane	0.009	0.54	1.09		[56]
	THF	0.52	0.16	0.84	0.16	[56]
	MeCN	0.025	0.06	0.15	0.85	[56]
m1H	*c*-Hexane	0.57	0.23	1.03		[65]
	THF	0.32				[65]
	CH_2Cl_2	0.29	0.38	1.05		[65]
	MeCN	0.17	0.42	1.01		[65]
m1Me	*c*-Hexane	0.56	0.22	1.00		[65]
	THF	0.22				[65]
	CH_2Cl_2	0.18	0.41	1.00		[65]
	MeCN	0.08	0.25	0.58		[65]
m1OM	*c*-Hexane	0.48	0.25	0.98		[65]
	THF	0.07	0.29	0.65	0.35	[65]
	CH_2Cl_2	0.05	0.20	0.45	0.55	[65]
	MeCN	<0.003	0.04	0.09	0.91	[65]
m1CN	*c*-Hexane	0.52	0.23	0.98		[65]
	THF	0.49				[65]
	CH_2Cl_2	0.42	0.27	0.96		[65]
	MeCN	0.37	0.32	1.01		[65]
o1H	*n*-Hexane	0.74	0.04	0.82		[57]
	CH_2Cl_2	0.92	0.01	0.94		[57]
	MeCN	0.86	0.08	1.02		[57]
o1Me	*n*-Hexane	0.75	0.05	0.85		[57]
	CH_2Cl_2	0.85	0.04	0.93		[57]
	MeCN	0.48	0.08	0.64		[57]
o1OM	*n*-Hexane	0.65	0.21	1.07		[57]
	CH_2Cl_2	0.22	0.11	0.44		[57]
	MeCN	0.0096	0.02	0.05		[57]
o1CN	*n*-Hexane	0.58	0.18	0.94		[57]
	CH_2Cl_2	0.65	0.10	0.85		[57]
	MeCN	0.71	0.08	0.87		[57]
p2	*n*-Hexane	0.62	0.16	0.94		[55]
	MeCN	0.95	0.01	0.97		[55]
p2-L1	*n*-Hexane	0.77	0.14	1.05		[58]
	MeCN	0.95	0.02	0.99		[58]
p2-L2	*n*-Hexane	0.68	0.25	1.18		[58]
	MeCN	0.95	0.08	1.11		[58]
p2-C1	CH_2Cl_2	<0.001	0.41	0.82		[58]
p2-C2	CH_2Cl_2	<0.001	0.44	0.88		[58]
m2	*n*-Hexane	0.17	0.34	0.85		[64]
	CH_2Cl_2	0.17	0.37	0.91		[64]
	MeCN	0.14	0.45	1.04		[64]
o2	*n*-Hexane	0.32	0.34	1.00		[57]
	CH_2Cl_2	0.74	0.18	1.10		[57]
	MeCN	0.71	0.17	1.05		[57]
p3H	*n*-Hexane	0.11	0.45	1.01		[52]
	CH_2Cl_2	0.23	0.44	1.11		[52]
	MeCN	0.35	0.33	1.01		[52]
p3Me	*n*-Hexane	0.18				[52]
	CH_2Cl_2	0.35	0.34	1.03		[52]
	MeCN	0.13	0.02	0.17	0.83	[52]
p3OM	*n*-Hexane	0.25	0.27	0.79		[52]
	CH_2Cl_2	0.06	<0.01	0.06	0.94	[52]
	MeCN	<0.005	<0.01	0.01	0.99	[52]
p3CN	*n*-Hexane	0.29				[52]
	CH_2Cl_2	0.22	0.34	0.9		[52]
	MeCN	0.27	0.30	0.87		[52]
p4MP	*n*-Hexane	0.33				[52]
4DNS	*c*-Hex	0.33	0.28	0.89		[69]
	Toluene	0.53	0.035	0.60	0.4	[69]
	THF	0.11	<0.01	<0.13	0.87	[69]
	CH_2Cl_2	0.008	<0.01	<0.03	0.97	[69]
	MeCN	<0.002	<0.01	<0.03	0.97	[69]
4DNS-**B3**	*n*-Hexane	0.21	0.38	0.97		[75]
	Toluene	0.31	0.08	0.47	0.53	[75]
	THF	0.07	0.01	0.09	0.91	[75]
	CH_2Cl_2	<0.005	<0.01	<0.03	0.97	[75]

Table 1 (*Continued*)

Compd.	Solvent	Φ_f	Φ_{tc}	$\Phi_f + 2\Phi_{tc}$	Φ_{TICT}	Ref.
	MeCN	<0.005	<0.01	<0.03	0.97	[75]
4DOS	*n*-Hexane	0.76	0.10	0.96		[62]
	CH_2Cl_2	0.61	0.20	1.01		[62]
4MPS	THF	0.73				[67]
4PPS	THF	0.45				[67]
17	*n*-Hexane	0.002	0.46	0.92		[80]
	THF	0.002	0.46	0.92		[80]
	MeCN	0.002	0.43	0.86		[80]
18	*n*-Hexane	0.10	0.49	1.08		[80]
	THF	0.035	0.46	0.93		[80]
	MeCN	0.056	0.48	0.97		[80]
19	*n*-Hexane	0.002	0.43	0.88		[80]
	THF	0.003	0.09	0.18	0.82	[80]
	MeCN	<0.001	0.01	0.02	0.98	[80]
20	*n*-Hexane	0.005	0.48	0.96		[80]
	THF	0.016	0.41	0.84		[80]
	MeCN	0.025	0.46	0.95		[80]
p-ABDI	*n*-Hexane	<0.001	0.45	0.90		[81]
	THF	<0.001	0.49	0.98		[81]
	MeCN	<0.001	0.50	1.00		[81]
m-ABDI	*n*-Hexane	0.34	0.37	1.08		[81]
	THF	0.28	0.35	0.98		[81]
	MeCN	0.16	0.45	1.06		[81]
p-HBDI	*n*-Hexane	<0.001	0.53	1.06		[81]
	THF	<0.001	0.46	0.92		[81]
	MeCN	<0.001	0.48	0.96		[81]

excited state with a small thermal barrier, except for those having a high C=C torsion barrier (≥7.0 kcal/mol) or undergoing efficient singlet-to-triplet intersystem crossing. If it is agreed that the photochemistry of *trans*- and *cis*-stilbenes has provided a good model for mechanistic understanding of the *cis*,*trans*-photoisomerization of alkenes, then we can say that *trans*-aminostilbenes are good models for understanding the formation and deactivation of the TICT state of D–A systems. We believe that the fluorescence-enhancing substituent effects and the TICT concepts gained from *trans*-aminostilbenes could be applied in many other systems of fundamentally or practically importance.

Acknowledgments

We would like thank MOST (NSC101-2113-M-002-005-MY3) and National Taiwan University (104R891303) for financial support and all the students and collaborators for their great contributions to the projects presented in this article.

Reference.

[1] Y. Zhang, G. Zhuang, M. Ouyang, B. Hu, Q. Song, J. Sun, C. Zhang, C. Gu, Y. Xu, Y. Ma, Mechanochromic and thermochromic fluorescent properties of cyanostilbene derivatives, Dyes Pigm. 98 (2013) 486–492.
[2] R. Anandakathir, U. Ojha, E.T. Ada, R. Faust, J. Kumar, Stilbene-based fluorescent sensor for detection of organophosphorus warfare nerve agents, J. Macromol. Sci. Pure Appl. Chem. 46 (2009) 1217–1222.
[3] X. Liu, X. Shu, X. Zhou, X. Zhang, J. Zhu, Ultra-sensitive fluorescent sensor for Hg^{2+} based on a donor–acceptor–donor framework, J. Phys. Chem. A 114 (2010) 13370–13375.
[4] J.-S. Yang, Y.-H. Lin, C.-S. Yang, Palladium-catalyzed synthesis of *trans*-4-(*N*,*N*-bis(2-pyridyl)amino) stilbene. A new intrinsic fluoroionophore for transition metal ions, Org. Lett. 4 (2002) 777–780.
[5] J.-S. Yang, C.-Y. Hwang, M.-Y. Chen, Bimodal fluorescence signaling based on control of the excited-state conformational twisting and the ground-state protonation processes, Tetrahedron Lett. 48 (2007) 3097–3102.
[6] C.-K. Lin, J.-S. Yang, Fluorescence response of TICT-active aminostilbenes to copper(II) ions: redox reaction vs ion recognition, Res. Chem. Itermed. 39 (2013) 19–32.
[7] M. Ono, A. Wilson, J. Nobrega, D. Westaway, P. Verhoeff, Z.-P. Zhuang, M.-P. Kung, H.F. Kung, 11C-labeled stilbene derivatives as Aβ-aggregate-specific PET imaging agents for Alzheimer's disease, Nuclear Med. Biol. 30 (2003) 565–571.
[8] S. Choi, D.S.T. Ong, J.W. Kelly, A stilbene that binds selectively to transthyretin in cells and remains dark until it undergoes a chemoselective reaction to create a bright blue fluorescent conjugate, J. Am. Chem. Soc. 132 (2010) 16043–16051.
[9] S. Bellow, G. Latouche, S.C. Brown, A. Poutaraud, Z.G. Cerovic, In vivo localization at the cellular level of stilbene fluorescence induced by *Plasmopara viticola* in grapevine leaves, J. Exp. Bot. (2012) .
[10] H.C. Li, Y.P. Lin, P.T. Chou, Y.M. Cheng, R.S. Liu, Color tuning and highly efficient blue emitters of finite diphenylamino-containing oligo(arylenevinylene) derivatives using fluoro substituents, Adv. Funct. Mater. 17 (2007) 520–530.
[11] C.-T. Chen, C.-L. Chiang, Y.-C. Lin, L.-H. Chan, C.-H. Huang, Z.-W. Tsai, C.-T. Chen, Ortho-substituent effect on fluorescence and electroluminescence of arylamino-substituted coumarin and stilbene, Org. Lett. 5 (2003) 1261–1264.
[12] S. Hwang, J.H. Lee, C. Park, H. Lee, C. Kim, C. Park, M.-H. Lee, W. Lee, J. Park, K. Kim, N.-G. Park, C. Kim, A highly efficient organic sensitizer for dye-sensitized solar cells, Chem. Commun. (2007) 4887–4889.
[13] Y.-D. Lin, C.-T. Chien, S.-Y. Lin, H.-H. Chang, C.-Y. Liu, T.J. Chow, Meta versus para substituent effect of organic dyes for sensitized solar cells, J. Photochem. Photobiol. A: Chem. 222 (2011) 192–202.
[14] Y.-D. Lin, T.J. Chow, Fluorine substituent effect on organic dyes for sensitized solar cells, J. Photochem. Photobiol. A: Chem. 230 (2012) 47–54.
[15] X. Wang, D. Wang, G. Zhou, W. Yu, Y. Zhou, Q. Fang, M. Jiang, Symmetric and asymmetric charge transfer process of two-photon absorbing chromophores: bis-donor substituted stilbenes, and substituted styrylquinolinium and styrylpyridinium derivatives, J. Mater. Chem. 11 (2001) 1600–1605.
[16] X.L.W.J.E. Ehrlich, I.-Y.S. Lee, Z.-Y. Hu, H. Röckel, S.R. Marder, J.W. Perry, Two-photon absorption and broadband optical limiting with bis-donor stilbenes, Opt. Lett. 22 (1997) 1843–1845.
[17] V.A. Svetlichnyi, Y.P. Meshalkin, Two-photon absorption and laser photolysis of trans-stilbene substitutes, Opt. Commun. 280 (2007) 379–386.
[18] T. Kogej, D. Beljonne, F. Meyers, J.W. Perry, S.R. Marder, J.L. Brédas, Mechanisms for enhancement of two-photon absorption in donor–acceptor conjugated chromophores, Chem. Phys. Lett. 298 (1998) 1–6.
[19] D. Beljonne, J.L. Brédas, M. Cha, W.E. Torruellas, G.I. Stegeman, J.W. Hofstraat, W.H.G. Horsthuis, G.R. Möhlmann, Two-photon absorption and third harmonic generation of di-alkyl-amino-nitro-stilbene (DANS): a joint experimental and theoretical study, J. Chem. Phys. 103 (1995) 7834–7843.
[20] M. Rumi, J.E. Ehrlich, A.A. Heikal, J.W. Perry, S. Barlow, Z. Hu, D. McCord-Maughon, T.C. Parker, H. Röckel, S. Thayumanavan, S.R. Marder, D. Beljonne, J.-L. Brédas, Structure–property relationships for two-photon absorbing chromophores: bis-donor diphenylpolyene and bis(styryl)benzene derivatives, J. Am. Chem. Soc. 122 (2000) 9500–9510.
[21] C.A. Stanier, S.J. Alderman, T.D.W. Claridge, H.L. Anderson, Unidirectional photoinduced shuttling in a rotaxane with a symmetric stilbene dumbbell, Angew. Chem. Int. Ed. 41 (2002) 1769–1772.
[22] W.-T. Sun, S.-L. Huang, H.-H. Yao, I.C. Chen, Y.-C. Lin, J.-S. Yang, An antilock molecular braking system, Org. Lett. 14 (2012) 4154–4157.
[23] J.R. Lakowicz, Principles of Fluorescence Spectroscopy, Springer Science + Business Media, New York, 2006205–208.
[24] D.H. Waldeck, Photoisomerization dynamics of stilbenes, Chem. Rev. 91 (1991) 415–436.
[25] H. Görner, H.J. Kuhn, *cis–trans* Photoisomerization of stilbenes and stilbene-like molecules, Adv. Photochem. 19 (1995) 1–117.
[26] H. Meier, The photochemistry of stilbenoid compounds and their role in materials technology, Angew. Chem. Int. Ed. Engl. 31 (1992) 1399–1420.
[27] J. Saltiel, Y.-P. Sun, Photochromism, molecules and systems, in: H. Dürr, H. Bouas-Laurent (Eds.), Photochromism, Molecules and Systems, Elsevier, Amsterdam, 1990, pp. 64–164.
[28] J. Saltiel, J.L. Charlton, Rearrangements in ground and excited states, in: P.D. Mayo (Ed.), Rearrangements in Ground and Excited States, Academic Press, New York, 1980, pp. 25–89.
[29] A.Y. Grumadas, Internal rotation in free molecules of styrene and *trans*-stilbene, J. Struct. Chem. 31 (1990) 19–24.
[30] G.B. Kistiakowsky, W.R. Smith, Kinetics of thermal *cis–trans* isomerization. III, J. Am. Chem. Soc. 56 (1934) 638–642.
[31] M.R. Ams, D. Ajami, S.L. Craig, J.-S. Yang, J. Rebek Jr., Control of stilbene conformation and fluorescence in self-assembled capsules, Beilstein J. Org. Chem. 5 (2009) 79.
[32] D. Tzeli, G. Theodorakopoulos, I.D. Petsalakis, D. Ajami, J. Rebek, Conformations and fluorescence of encapsulated stilbene, J. Am. Chem. Soc. 134 (2012) 4346–4354.
[33] D.C. Todd, G.R. Fleming, *Cis*-stilbene isomerization: temperature dependence and the role of mechanical friction, J. Chem. Phys. 98 (1993) 269–279.
[34] H. Görner, Phosphorescence of *trans*-stilbene, stilbene derivatives, and stilbene-like molecules at 77 K, J. Phys. Chem. 93 (1989) 1826–1832.
[35] J. Saltiel, A. Marinari, D.W.L. Chang, J.C. Mitchener, E.D. Megarity, *Trans–cis* photoisomerization of the stilbenes and a reexamination of the positional dependence of the heavy-atom effect, J. Am. Chem. Soc. 101 (1979) 2982–2996.
[36] J.-S. Yang, Y.-T. Huang, J.-H. Ho, W.-T. Sun, H.-H. Huang, Y.-C. Lin, S.-J. Huang, S.-L. Huang, H.-F. Lu, I. Chao, A pentiptycene-derived light-driven molecular brake, Org. Lett. 10 (2008) 2279–2282.

[37] W.-T. Sun, G.-J. Huang, S.-L. Huang, Y.-C. Lin, J.-S. Yang, A light-gated molecular brake with antilock and fluorescence turn-on alarm functions: application of singlet-state adiabatic *cis* → *trans* photoisomerization, J. Org. Chem. 79 (2014) 6321–6325.
[38] E. Lippert, W. Lüder, H. Boos, Advances in molecular spectroscopy, in: A. Mangini (Ed.), Advances in Molecular Spectroscopy, Oxford, Pergamon, 1962, pp. 443–457.
[39] W. Rettig, E. Lippert, Twisting relaxation and dual fluorescence of *p*-*N*,*N*-dialkylaminobenzonitriles, J. Mol. Struct. 61 (1980) 17–22.
[40] W. Schuddeboom, S.A. Jonker, J.M. Warman, U. Leinhos, W. Kuehnle, K.A. Zachariasse, Excited-state dipole moments of dual fluorescent 4-(dialkylamino) benzonitriles: influence of alkyl chain length and effective solvent polarity, J. Phys. Chem. 96 (1992) 10809–10819.
[41] Z.R. Grabowski, K. Rotkiewicz, W. Rettig, Structural changes accompanying intramolecular electron transfer: focus on twisted intramolecular charge–transfer states and structures, Chem. Rev. 103 (2003) 3899–4032.
[42] E. Abraham, J. Oberlé, G. Jonusauskas, R. Lapouyade, C. Rullière, Dual excited states in 4-dimethylamino 4′-cyanostilbene (DCS) revealed by sub-picosecond transient absorption and Kerr ellipsometry, J. Photochem. Photobiol. A: Chem. 105 (1997) 101–107.
[43] W. Rettig, W. Majenz, Competing adiabatic photoreaction channels in stilbene derivatives, Chem. Phys. Lett. 154 (1989) 335–341.
[44] E. Gilabert, R. Lapouyade, C. Rullière, Dual fluorescence in *trans*-4-dimethylamino-4′-cyanostilbene revealed by picosecond time-resolved spectroscopy: a possible new TICT compound, Chem. Phys. Lett. 145 (1988) 262–268.
[45] R. Lapouyade, K. Czeschka, W. Majenz, W. Rettig, E. Gilabert, C. Rulliere, Photophysics of donor-acceptor substituted stilbenes. A time-resolved fluorescence study using selectively bridged dimethylamino cyano model compounds, J. Phys. Chem. 96 (1992) 9643–9650.
[46] J.F. Letard, R. Lapouyade, W. Rettig, Structure–photophysics correlations in a series of 4-(dialkylamino) stilbenes: intramolecular charge transfer in the excited state as related to the twist around the single bonds, J. Am. Chem. Soc. 115 (1993) 2441–2447.
[47] Y.V. Il'ichev, W. Kühnle, K.A. Zachariasse, Photophysics of 4-dimethylamino-4′-cyanostilbene and 4-azetidinyl-4′-cyanostilbene. Time-resolved fluorescence and *trans*–*cis* photoisomerisation, Chem. Phys. 211 (1996) 441–453.
[48] S.A. Kovalenko, R. Schanz, T.A. Senyushkina, N.P. Ernsting, Femtosecond spectroscopy of *p*-dimethylaminocyanostilbene in solution-no evidence for dual fluorescence, Phys. Chem. Chem. Phys. 4 (2002) 703–707.
[49] N. Eilers-König, T. Kühne, D. Schwarzer, P. Vöhringer, J. Schroeder, Femtosecond dynamics of intramolecular charge transfer in 4-dimethylamino-4′-cyanostilbene in polar solvents, Chem. Phys. Lett. 253 (1996) 69–76.
[50] K. Rechthaler, G. Köhler, Photophysical properties of a highly fluorescent push–pull stilbene, Chem. Phys. Lett. 250 (1996) 152–158.
[51] J.-S. Yang, K.-L. Liau, C.-M. Wang, C.-Y. Hwang, Substituent-dependent photoinduced intramolecular charge transfer in *N*-aryl-substituted trans-4-aminostilbenes, J. Am. Chem. Soc. 126 (2004) 12325–12335.
[52] J.-S. Yang, K.-L. Liau, C.-Y. Hwang, C.-M. Wang, Photoinduced single- versus double-bond torsion in donor–acceptor-substituted *trans*-stilbenes, J. Phys. Chem. A 110 (2006) 8003–8010.
[53] U. Leinhos, W. Kuehnle, K.A. Zachariasse, Intramolecular charge transfer and thermal exciplex dissociation with *p*-aminobenzonitriles in toluene, J. Phys. Chem. 95 (1991) 2013–2021.
[54] F.D. Lewis, R.S. Kalgutkar, J.-S. Yang, The photochemistry of *trans-ortho-*, *-meta-*, and *-para*-aminostilbenes, J. Am. Chem. Soc. 121 (1999) 12045–12053.
[55] J.-S. Yang, S.-Y. Chiou, K.-L. Liau, Fluorescence enhancement of *trans*-4-aminostilbene by *N*-phenyl substitutions: the amino conjugation effect, J. Am. Chem. Soc. 124 (2002) 2518–2527.
[56] J.-S. Yang, C.-K. Lin, A.M. Lahoti, C.-K. Tseng, Y.-H. Liu, G.-H. Lee, S.-M. Peng, Effect of ground-state twisting on the *trans* → *cis* photoisomerization and TICT state formation of aminostilbene, J. Phys. Chem. A 113 (2009) 4868–4877.
[57] C.-K. Lin, C. Prabhakar, J.-S. Yang, *o*-Amino conjugation effect on the photochemistry of *trans*-aminostilbenes, J. Phys. Chem. A 115 (2011) 3233–3242.
[58] C.-J. Lin, Y.-H. Liu, S.-M. Peng, J.-S. Yang, Photoluminescence and *trans* → *cis* photoisomerization of aminostyrene-conjugated phenylpyridine C^N ligands and their complexes with platinum(II): the styryl position and the amino substituent effects, J. Phys. Chem. B 116 (2012) 8222–8232.
[59] F.D. Lewis, J.-S. Yang, The excited state behavior of aminostilbenes. A new example of the meta effect, J. Am. Chem. Soc. 119 (1997) 3834–3835.
[60] K.J. Smit, K.P. Ghiggino, Influence of solvent on the photochemistry of 4,4′-diaminostilbene, Chem. Phys. Lett. 122 (1985) 369–374.
[61] Y. Sutovsky, G.I. Likhtenshtein, S. Bittner, Synthesis and photochemical behavior of donor–acceptor systems obtained from chloro-1,4-naphthoquinone attached to *trans*-aminostilbenes, Tetrahedron 59 (2003) 2939–2945.
[62] K.-L. Liau, Studies on the Photoinduced Intramolecular Charge Transfer Behavior of *para*- and *meta*-Aminostilbenes, Department of Chemistry, National Central University, Tauyuan, 2007.
[63] F.D. Lewis, W. Weigel, X. Zuo, Relaxation pathways of photoexcited diaminostilbenes. The *meta*-amino effect, J. Phys. Chem. A 105 (2001) 4691–4696.
[64] J.-S. Yang, K.-L. Liau, C.-W. Tu, C.-Y. Hwang, Excited-state behavior of *N*-phenyl-substituted *trans*-3-aminostilbenes:where the *m*-amino effect meets the amino-conjugation effect, J. Phys. Chem. A 109 (2005) 6450–6456.
[65] J.-S. Yang, K.-L. Liau, C.-Y. Li, M.-Y. Chen, Meta conjugation effect on the torsional motion of aminostilbenes in the photoinduced intramolecular charge–transfer state, J. Am. Chem. Soc. 129 (2007) 13183–13192.
[66] F.D. Lewis, W. Weigel, Excited state properties of donor–acceptor substituted *trans*-stilbenes: the *meta*-amino effect, J. Phys. Chem. A 104 (2000) 8146–8153.
[67] J.-S. Yang, J.-L. Yan, Synthesis and properties of triptycene-diaminostilbene hybrid systems, J. Chin. Chem. Soc. 53 (2006) 1509–1516.
[68] H.E. Zimmerman, *Meta-ortho* effect in organic photochemistry: mechanistic and exploratory organic photochemistry, J. Phys. Chem. A 102 (1998) 5616–5621.
[69] H. Gruen, H. Görner, *Trans* → *cis* photoisomerization, fluorescence, and relaxation phenomena of *trans*-4-nitro-4′-(dialkylamino) stilbenes and analogues with a nonrotatable amino group, J. Phys. Chem. 93 (1989) 7144–7152.
[70] R. Lapouyade, A. Kuhn, J.-F. Letard, W. Rettig, Multiple relaxation pathways in photoexcited dimethylaminonitro- and dimethylaminocyano-stilbenes, Chem. Phys. Lett. 208 (1993) 48–58.
[71] S.A. Kovalenko, R. Schanz, V.M. Farztdinov, H. Hennig, N.P. Ernsting, Femtosecond relaxation of photoexcited *para*-nitroaniline: solvation, charge transfer, internal conversion and cooling, Chem. Phys. Lett. 323 (2000) 312–322.
[72] R. Farztdinov, S.A. Schanz, Relaxation of optically excited *p*-nitroaniline: semiempirical quantum-chemical calculations compared to femtosecond experimental results, J. Phys. Chem. A 104 (2000) 11486–11496.
[73] S. Rafiq, R. Yadav, P. Sen, Femtosecond excited-state dynamics of 4-nitrophenyl pyrrolidinemethanol: evidence of twisted intramolecular charge–transfer and intersystem crossing involving the nitro group, J. Phys. Chem. A 115 (2011) 8335–8343.
[74] R. Ghosh, D.K. Palit, Ultrafast dynamics of the excited states of 1-(*p*-nitrophenyl)-2-(hydroxymethyl) pyrrolidine, J. Phys. Chem. A 116 (2012) 1993–2005.
[75] C.-K. Lin, Y.-F. Wang, Y.-C. Cheng, J.-S. Yang, Multisite constrained model of *trans*-4-(*N*,*N*-dimethylamino)-4′-nitrostilbene for structural elucidation of radiative and nonradiative excited states, J. Phys. Chem. A 117 (2013) 3158–3164.
[76] H. Bässler, B. Schweitzer, Site-selective fluorescence spectroscopy of conjugated polymers and oligomers, Acc. Chem. Res. 32 (1998) 173–182.
[77] J.-S. Yang, Y.-D. Lin, Y.-H. Lin, F.-L. Liao, Zn(II)-induced ground-state π-deconjugation and excited-state electron transfer in *N*,*N*-bis(2-pyridyl) amino-substituted arenes, J. Org. Chem. 69 (2004) 3517–3525.
[78] J.-S. Yang, Y.-D. Lin, Y.-H. Chang, S.-S. Wang, Synthesis, dual fluorescence, and fluoroionophoric behavior of dipyridylaminomethylstilbenes, J. Org. Chem. 70 (2005) 6066–6073.
[79] J.-S. Yang, C.-Y. Hwang, C.-C. Hsieh, S.-Y. Chiou, Spectroscopic correlations between supermolecules and molecules. Anatomy of the ion-modulated electronic properties of the nitrogen donor in monoazacrown-derived intrinsic fluoroionophores, J. Org. Chem. 69 (2004) 719–726.
[80] G.-J. Huang, J.-S. Yang, The *N*-arylamino conjugation effect in the photochemistry of fluorescent protein chromophores and aminostilbenes, Chem. Asian J. 5 (2010) 2075–2085.
[81] J.-S. Yang, G.-J. Huang, Y.-H. Liu, S.-M. Peng, Photoisomerization of the green fluorescence protein chromophore and the *meta*- and *para*-amino analogues, Chem. Commun. (2008) 1344–1346.

Jye-Shane Yang received his PhD degree from Northwestern University (with F. D. Lewis) in 1997. He then joined T. M. Swager's group as a postdoctoral associate at Massachusetts Institute of Technology. He started his independent research at National Central University, Taiwan in 1998. In 2005, he moved back to his alma mater, National Taiwan University and was promoted to a full professor in 2007. Since 2013, he has been a distinguished professor and the departmental head. His current research interests include photochemistry and photophysics of donor–acceptor molecules, light- and redox-gated artificial molecular switches and motors, and electronic properties of metal-containing and metal-free π-conjugated molecular systems.

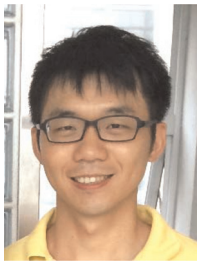

Che-Jen Lin received his master degree from National Taiwan University (NTU) in 2009 (with J.-S. Yang). After one-year military service, he served as a teaching and research assistant at NTU for two years. He has been a PhD student in Prof. J.-S. Yang's group since 2012. His research interest is photophysics and photochemistry of organic and organometallic π-conjugated systems.